

NUMERICAL SIMULATION OF FLOW OF SHEAR-THINNING FLUIDS IN
CORRUGATED CHANNELS

A Thesis

by

ROHIT AIYALUR SHANKARAN

Submitted to the Office of Graduate Studies of
Texas A&M University
in partial fulfillment of the requirements for the degree of

MASTER OF SCIENCE

December 2007

Major Subject: Mechanical Engineering

NUMERICAL SIMULATION OF FLOW OF SHEAR-THINNING FLUIDS IN
CORRUGATED CHANNELS

A Thesis

by

ROHIT AIYALUR SHANKARAN

Submitted to the Office of Graduate Studies of
Texas A&M University
in partial fulfillment of the requirements for the degree of

MASTER OF SCIENCE

Approved by:

Chair of Committee,	K. R. Rajagopal
Committee Members,	N. K. Anand
	Hamn-Ching Chen
Head of Department,	Dennis L. O'Neal

December 2007

Major Subject: Mechanical Engineering

ABSTRACT

Numerical Simulation of Flow of Shear-Thinning Fluids
in Corrugated Channels. (December 2007)

Rohit Aiyalur Shankaran, B. E, Osmania University

Chair of Advisory Committee: Dr. K. R. Rajagopal

A numerical study of flow of a shear thinning fluid through a pair of corrugated plates was carried out. The aim of the study was to observe and understand the behavior of the flow of shear thinning fluids through channels where the fluid is subjected to a periodic increase and decrease in cross-section area. Such conditions are frequently observed in the flow of blood through blood vessels, movement of lubricating oils through the ground during the oil extraction process, in the process industry. Since we are dealing with non-Newtonian fluids the non-linear terms in the constitutive equation have a significant affect on their behavior.

The plates modeled for the study had a sinusoidal profile. A total of four different plates were with varying amplitude and wavelengths were simulated. The simulations were done both in two and three dimensional space. A wide range of Reynolds numbers were used for each plate. The Reynolds number used was a function of the half the average plate spacing (h) and the velocity. The range of Reynolds numbers used is 100 to 1000. The velocity profiles along the crest, trough and center lines were generated.

It was observed that even at low velocities and low Reynolds numbers the shear stress at the wall was significant. It was also observed that even at low velocities and low Reynolds numbers reversed flow can occur near the regions where the profile of geometry is sinusoidal. Such behavior is a characteristic of shear thinning fluid.

To my loving sister, parents and friends

ACKNOWLEDGEMENTS

I would like to thank my advisor Dr. K. R. Rajagopal for his great support and giving me an opportunity to work with him over the last two years. I have learned to appreciate the topics he has taught me from a new perspective and gained a great amount of knowledge in the process. He has been a great Inspiration to me.

I would like to thank Dr. N. K. Anand and Dr. H. C. Chen for being on my committee and also for their help and support. I have gained a lot of knowledge from them in the area of numerical methods.

I would also like to thank some of the professors in Mechanical and Civil engineering with whom I have taken courses and learnt new concepts and gained a lot of knowledge.

I would also like to thank my parents for their great love and support throughout my life. I would like to thank them for having faith and confidence in me to do well, I am very grateful to them. I would like to thank my sister Nandini for her love and support through the years. I would also like to thank some of my friends, Prakash, Preetish, Nikhil, Trijya, Sai, Stephen, Jawahar, Richa, Sonu and Vineet for their great support. I would like to thank my past and present colleagues in my research group, Sarathy, Sai, Waqar, Parag, Srivatsan and Sriram for all the help they have provided. I learned a lot from them and they always helped me when I had difficulties with my research.

I would also like to thank Texas A&M University for giving me an opportunity to pursue my higher education at such a prestigious institution. The facilities available at Texas A&M are of very high standard and the help from the supercomputing facility has been vital, without which I would not have been able to run my simulations so quickly and efficiently.

NOMENCLATURE

\mathbf{V}	Velocity vector
\mathbf{T}	Stress tensor
P	Hydrodynamic pressure
\mathbf{I}	Identity
μ	Dynamic viscosity
\underline{D}	Symmetric part of the velocity gradient
ε	Internal energy
q	Heat flux vector
r	Heat being radiated
t	Time
ν	Kinematic viscosity
ρ	Density of the fluid
Div	Divergence
Grad	Gradient
\underline{L}	Velocity Gradient

TABLE OF CONTENTS

	Page
ABSTRACT.....	iii
ACKNOWLEDGEMENTS	v
NOMENCLATURE	vi
TABLE OF CONTENTS	vii
LIST OF FIGURES	ix
LIST OF TABLES	xi
1. INTRODUCTION	1
1.1 Applications Of Non-Newtonian Fluids	2
1.2 Classification Of Non-Newtonian Fluids.....	3
1.2.1 Time-Independent Behavior	4
1.2.1 Time-Independent Behavior	4
1.2.1.1 Shear-Thinning Fluids	4
1.2.1.2 Power-Law Model	5
1.2.1.3 Cross Model.....	5
1.2.1.4 The Carreau Model	6
1.2.1.5 Viscoplastic Fluids.....	6
1.2.1.6 Shear-Thickening Fluids.....	7
1.2.2 Time-Dependant Behavior.....	7
1.2.2.1 Thixotropy.....	8
1.2.2.2 Rheopexy	8
1.2.3 Viscoelastic Behavior In Fluids.....	8
1.3 Previous Work	8
2. KINEMATICS.....	10
2.1 Continuum Assumption	10
2.2 kinematics	11
2.3 Balance Of Mass	13
2.3.1 Eulerian Approach	13
2.3.2 Lagrangian Approach.....	14
2.4 Balance Of Linear Momentum	14
2.5 Balance Of Energy	14
3. CONSTITUTIVE EQUATIONS.....	16
3.1 Non-Dimensionalization	20
4. PROBLEM DESCRIPTION AND PROCEDURE	21
4.1 Procedure For Numerical Simulation	24
5. NUMERICAL SIMULATION.....	28

	Page
5.1 Fluent	28
5.2 Running Fluent And Gambit.....	29
5.3 Gambit.....	29
5.4 Geometry.....	30
5.5 Meshing.....	30
5.5.1 Specifying Zone Type.....	32
5.5.2 Boundary Layers.....	33
5.6 The Fluent Process.....	33
5.7 Steps In Solving A CFD Problem.....	35
5.8 Setting Boundary Types.....	35
5.8.1 Mass Flow Boundary Condition	36
5.8.1 Mass Flow Boundary Condition	36
5.8.2 Wall Boundary Conditions	37
5.9 Shear-Stress Calculation At Wall Boundaries	38
5.10 Shear-Stress Calculation In Laminar Flow	38
5.11 Defining Materials	38
5.12 Material Types And Databases	39
5.13 Viscosity	39
5.14 The Solver.....	40
5.15 User Defined Functions	42
6. RESULTS AND CONCLUSIONS	45
6.1 Plate 1.....	45
6.2 Plate 2.....	51
6.3 Plate 3.....	54
6.4 Plate 4.....	56
REFERENCES	62
VITA	64

LIST OF FIGURES

FIGURE	Page
2.1. Motion of a Body	11
2.2. Body in the Current Configuration	13
4.1. Schematic Diagram of a Plate	22
4.2. Plates Aligned with Each Other Without Any Phase Difference	23
4.3. Plates Aligned with a Phase Difference of 45°	23
4.4. Plates Aligned with a Phase Difference of 90°	23
4.5. Schematic Diagram Showing the Crest Line and the Trough Line	24
4.6. Boundary and Zone Types	25
4.7. Two-Dimensional Mesh	25
5.1. Structure of Fluent Program	29
5.2. Types of Elements Used in Gambit	35
6.1. Velocity Contours, Blood, $a = 0.0022$, $\lambda = 0.1016$, $Re = 1000$	45
6.2. Plate 1, Centerline Velocity Profile, Blood	46
6.3. Plate 1 Velocity Vectors, Oil, $a = 0.0022$, $\lambda = 0.1016$, $Re = 1000$	47
6.4. Plate 1, Oil, $Re = 1000$, Centerline Velocity Profile	47
6.5. Velocity Profile at Trough Line, Oil, $Re = 1000$	48
6.6. Velocity Profile at Trough Line, Oil, $Re = 500$	49
6.7. Plate 1, Velocity Vectors, Oil, $Re = 100$	49
6.8. Velocity Contours, Phase 45° , Oil, $a = 0.0022$, $\lambda = 0.1016$, $Re = 1000$	50
6.9. Velocity Contours, Oil, $a = 0.0022$, $\lambda = 0.0254$, $Re = 1000$	51
6.10. Plate 2, Centerline Velocity Profile	52
6.11. Velocity Vectors, Phase 0, Oil, $a = 0.0022$, $\lambda = 0.0254$, $Re = 1000$	53
6.12. Velocity Contours, Phase 90° , Oil, $a = 0.0022$, $\lambda = 0.0254$, $Re = 1000$	54
6.13. Velocity Vectors, Phase 90° , Oil, $a = 0.0022$, $\lambda = 0.0254$, $Re = 1000$	54
6.14. Velocity Contours, Phase 0, Oil, $a = 0.0005$, $\lambda = 0.0254$, $Re = 1000$	55
6.15. Velocity Vectors, Phase 0, Oil, $a = 0.0005$, $\lambda = 0.0254$, $Re = 1000$	55
6.16. Velocity Vectors, Phase 0, Oil, $a = 0.0044$, $\lambda = 0.1016$, $Re = 1000$	56
6.17. Plate 4, Centerline Velocity Profile	57

FIGURE	Page
6.18. Velocity Vectors, Oil, $a = 0.0044$, $\lambda = 0.1016$, $Re = 100$	57
6.19. Velocity Vectors, Phase 45° , Oil, $a = 0.0044$, $\lambda = 0.1016$, $Re = 1000$	58
6.20. Velocity Vectors, Phase 45° , Oil, $a = 0.0044$, $\lambda = 0.1016$, $Re = 1000$	59
6.21. Velocity Vectors, Phase 90° , Oil, $a = 0.0044$, $\lambda = 0.1016$, $Re = 1000$	59
6.22. Velocity Vectors, Phase 90° , Oil, $a = 0.0044$, $\lambda = 0.1016$, $Re = 1000$	60
6.23. Velocity Vectors, Phase 90° , Blood, $a = 0.0044$, $\lambda = 0.1016$, $Re = 1000$	61

LIST OF TABLES

TABLE	Page
4.1. Plate Dimensions	21
4.2. Material Properties.....	26

1. INTRODUCTION

A fluid which cannot be expressed using the Navier-Stokes Equations is a non-Newtonian fluid.

Most of fluids we encounter in physical and industrial processes, other than air and water are non-Newtonian in nature. There is a growing importance attached to understanding the behavior of non-Newtonian fluids in the polymer, petroleum, food processing industries. It's especially important to understand the flow of non-Newtonian fluids thorough geometries where the cross section through which the fluid flows varies. The following sections try to address some of these concerns. It is shown for example that in non-Newtonian fluids there can be reversed flow even at low Reynolds' numbers. Such a property might be undesirable in many applications. Often rheology arises because the fluid in question builds up a microstructure at the molecular level which becomes sufficiently extensive to affect the macroscopic properties of the fluid, Schwarz [14]. In lava, for example, the microstructure is provided by a network of interlocked silicate crystals, and endows the fluid with an internal strength that allows lava to withstand a certain amount of imposed stress before it flows.

Understanding of Non-Newtonian fluid mechanics has grown only recently compared to Newtonian fluid mechanics. The origin of Non-Newtonian fluid mechanics could be attributed to the need to understand the relationship between bulk-flow of polymers to their molecular structure, James [7-8]. The definition of a non-Newtonian fluid given earlier is quite a negative one. Hence there is need for a classification of the various types of non-Newtonian fluid behavior.

Non-Newtonian behavior is generally observed in concentrated suspensions and high molecular weight materials. Many household items that exhibit such behavior include

dough, whipped cream, butter, salad dressing, ketchup, egg white. Non-Newtonian behavior is a characteristic of polymer solutions. Non-Newtonian behavior for instance is observed in the industry during the production of synthetic fiber such as nylon, during the drawing process. Even the motion of mountain ranges, sediment beds and magma are governed by rheology. Non-Newtonian materials are often referred to as Viscoelastic materials because they exhibit properties of an elastic solid and a viscous fluid, Sureshkumar [15].

Most biological fluids contain high molecular weight components and hence exhibit rheological behavior. Blood for example is a very widely studied non-Newtonian fluid. It consists of erythrocytes which constitutes to above 40% of the volume and the protein in the suspending fluid has a high molecular weight, making it non-Newtonian. These two components make blood a rheologically complex material. The other important body fluids which are non-Newtonian are mucous which is a respiratory fluid and synovial fluid which is present in the joints. Mucous in the respiratory system plays a very important role in maintaining proper respiratory behavior, hence understanding its rheological properties are very important.

Research on flow between corrugated plates is originally motivated by the strong non-Newtonian effects observed in flows involving porous media.

1.1 Applications Of Non-Newtonian Fluids

Non-Newtonian fluids includes a lot of industrial lubricants, many fluids that are pumped into oil wells to improve oil recovery, and some fluids like blood that are important in biology. Due to the advantages that result from the non-Newtonian behavior of polymer melts and solutions, polymer processing has become a huge industry for the manufacture of artificial fiber. The fiber is made by drawing molten polymer through a dye and then stretching it while being cooled. The importance of non-Newtonian fluid mechanics in the polymerization process is immense. The viscosity of the polymer changes from 10^{-2} to 10^6 poise. Elastic stresses in polymeric and other complex fluids can give rise to strange

flow behavior not seen in Newtonian fluids. This can, for example, produce undesirable instabilities in industrial processes.

Understanding Non-Newtonian behavior of polymers could be of great importance in improving their quality. Understanding materials used for Coating of surfaces, like paint can very helpful in determining its brushability. If it's too viscous it could leave brush marks and if too thin it would not coat the surface sufficiently.

The petroleum industry uses a lot of materials that are non-Newtonian. Drilling muds for example are used as a lubricant. So it is important for these muds to have low viscosity under shearing and high viscosity at rest. Such a material is termed as a shear thinning material. Lots of foods used in the food processing industry are non-Newtonian in nature. On offshore platforms it is very common to find fluids of a non-Newtonian nature flowing through corrugated channels. The reason for this is that the channels are designed to be corrugated in an attempt to break up boundary layers, Rajagopal [13].

1.2 Classification Of Non-Newtonian Fluids

A non-Newtonian fluid is one which cannot be defined using the Navier-Stokes Equations. Such a fluid exhibits non-equal normal stress in a simple shearing flow. The value of viscosity instead depends on flow conditions, such as flow geometry, shear stress or shear rate developed within the fluid and time for which the shear stress is applied among other factors.

There are three categories into which non-Newtonian fluids are classified.

1. Generalized Newtonian fluids: The rate of shear of the fluid is dependent only on the current value of the shear stress. These are also called purely viscous or time-independent fluids.
2. Materials for which the shear stress and rate of shear depends on the time for which the shear is applied. These materials are therefore time dependent.

3. Materials which exhibit properties of both elastic solids and viscous fluids. These materials are called Viscoelastic. In such materials there is only a partial recovery to the original state when a deformation or stress is applied.

There are also materials which have properties that are a combination of the three properties mentioned above. There are also materials that are either elastic solids or viscous fluids depending on the prevailing conditions.

1.2.1 Time-Independent Behavior

This type of fluid behavior can be further subdivided into three types: Shear-thinning fluids, Viscoplastic fluids and Dilatant fluids.

1.2.1.1 Shear-Thinning Fluids

In Shear-thinning or pseudoplastic fluids the viscosity decreases with an increase in rate of shear. The decrease in viscosity varies for different fluids. It has been observed in polymer solutions that the viscosity is constant at very low and very high rates of shear. The terms zero-shear viscosity and infinite shear viscosity used for the viscosity at low and high rate of shear respectively. Lower molecular weight polymers have a wider range in which the viscosity is constant. Shear-thinning fluids are the most common type of non-Newtonian fluids encountered. They are also the focus of the research in question. Some of the models used for modeling Shear-thinning fluids are discussed below.

There are quite a few models that can be used to model Shear-thinning fluids. Some of the models like the power-Law and the Carreau model use curve-fitting, while the others like the Eyring model have more of a theoretical approach based on statistical mechanics.

1.2.1.2 Power-Law Model

This model is also known as the Ostwald-De Waele model. It is a model that can be used to model pseudoplastic fluids. In this model the shear stress is written as a power of shear rate. The model uses two curve fitting parameters, one called the power law index and the other is generally referred to as fluid consistency coefficient.

$$\tau_{yx} = k * \left(\frac{du}{dy} \right)^n \quad (1.1)$$

Here τ_{yx} (N/m²) is the shear stress, $\frac{du}{dy}$ (s⁻¹) is the rate of shear, k (N/m².sⁿ) is flow consistency index and n is the power law index. k and n are the curve fitting parameters. This is a generalized equation and the nature of the fluid determines the value of the power law index. For a Shear-thinning fluids n is less than 1 (lower the value of n below 1 greater the degree of shear-thinning), it is 1 for a Newtonian fluid and greater than 1 for dilatant fluids. Its simplicity is the main reason for its wide usage. But generally the values of k and n are dependent on the rate of shear and its prediction of the zero and infinite values of viscosity can be inaccurate. The values of k and n are also affected by temperature.

1.2.1.3 Cross Model

It is based on the assumption that shear-thinning behavior is caused by formation and breakage of structural units in the material. The equation for the cross model is given below.

$$\frac{\mu - \mu_{\infty}}{\mu_0 - \mu_{\infty}} = \frac{1}{1 + (\lambda \dot{\gamma}_{xy})^{2/3}} \quad (1.2)$$

As discussed before the constants μ_0 and μ_{∞} are the zero and infinite shear viscosities respectively. λ is a time constant and $\dot{\gamma}_{xy} = \frac{du}{dy}$ is the rate of shear. This model works well for a variety of shear-thinning fluids. There have also been variants where the 2/3 in the equation is replaced with a parameter which is calculated by curve fitting.

1.2.1.4 The Carreau Model

It is a widely used and effective model for shear-thinning fluids. The Carreau model tries to describe a wide range of fluids through a curve-fit that pieces together functions for both Newtonian and shear-thinning non-Newtonian fluids.

$$\frac{\mu - \mu_{\infty}}{\mu_0 - \mu_{\infty}} = \left[1 + \left(\lambda * \frac{du}{dy} \right)^2 \right]^{(n-1)/2} \quad (1.3)$$

Where, the constants μ_0 and μ_{∞} are the zero and infinite shear viscosities respectively. λ is a time constant and $\frac{du}{dy}$ is the rate of shear. n is less than 1 for shear-thinning fluids.

1.2.1.5 Viscoplastic Fluids

These types of fluids resist any deformation initially and deform or flow only when the applied stress exceeds a critical value which is sometimes referred to as yield stress. Beyond the point of the yield stress the behavior of the flow curve could be linear or non-linear. A fluid which has got a linear flow pattern beyond the point of the yield stress is known as a Bingham plastic fluid. It behaves as a rigid body at low stresses. It has applications in mathematical modeling of mud flow in off shore engineering.

$$\frac{\partial u}{\partial y} = 0 \text{ if } \tau < \tau_0 \quad (1.4)$$

$$\frac{\partial u}{\partial y} = \frac{(\tau - \tau_0)}{\mu} \text{ if } \tau > \tau_0 \quad (1.5)$$

Various models like the Bingham plastic model, Casson Model and The Herschel-Bulkley Model are available for modelling such viscoplastic flows.

1.2.1.6 Shear-Thickening Fluids

In these materials the viscosity increases with an increase in the rate of shear. Such fluids are also called dilatant fluids. Such behavior is observed in concentrated suspensions of solids.

This phenomenon of the viscosity increasing with the rate of shear is explained in the following way. When a suspension of fluid in a solid is considered at rest, the voids between the solid particles is minimal because of all the fluid particles filling the spaces, thereby providing good lubrication for the movement of the solid particles. The same behavior is observed at low rates of shear. When such a suspension is subjected to high rates of shear there is a slight expansion of the material because of the breakage of the dense packing of solid particles. Thus the liquid is no longer sufficient to fill the voids between the solid particles which results in friction between the solid particles. This results in a rapid increase in the stress causing an increase in viscosity. Due to a lack or minimal usage of such materials in the industry there has been little research on them until recently. But of late, there has been a lot of interest in studying such materials with the usage of highly loaded systems in the processing industry.

1.2.2 Time-Dependant Behavior

Shear flow properties depend on both rate and time for shearing for most materials. Many construction materials and food-stuffs exhibit such properties. When they are sheared at a constant rate of shear followed by a period of rest their apparent viscosity gradually decreases as their internal structure breaks down progressively. With time the change in viscosity drops to zero at which point a state of equilibrium is reached. This type of fluid behavior is divided into two categories, namely Thixotropy and negative Thixotropy.

1.2.2.1 Thixotropy

Thixotropy is a property of a material in which its apparent viscosity or shear stress decreases with time when it is subjected to a constant rate of shear.

1.2.2.2 Rheopexy

Materials for which the apparent viscosity increases with the duration of shearing are said to exhibit Rheopexy. There are very few materials that exhibit such behavior.

1.2.3 Viscoelastic Behavior In Fluids

Viscoelastic materials show properties of both elastic solids and viscous fluids under different conditions. Perfectly viscous flow and elastic deformation are the limiting cases for a Viscoelastic material. Many materials like polymer melts and solutions, soap solutions and asphalt exhibit Viscoelastic properties. When stress is applied to viscoelastic materials and released, the applied stress gradually relaxes unlike an elastic solid where the stress relaxes immediately or a viscous fluid where it never relaxes. A similar response is observed when a strain is applied.

1.3 Previous Work

There has been a lot of study on flow of non-Newtonian fluids through channels. But very few of these deal with the flow of non-Newtonian fluids through corrugated channels, Lee [9], Yalamanchili, Sirivat and Rajagopal [16], Yalamanchili [17]. A few of them are discussed in the next section.

A numerical study of a two-dimensional steady developing fluid flow and heat transfer through a periodic wavy passage for a fluid with a Prandtl number of 0.7 was carried out by Bahaidarah, Anand and Chen [1]. The results were compared to flow through a corresponding straight channel. Sinusoidal and arc-shaped configurations were studied for a range of geometric parameters. The fluids studied were Newtonian.

There was study of flow of water in turbulent flow through a channel done by Hanratty [2-3]. The bottom plate was sinusoidal while the top was flat. The velocity profiles, pressure and shear stress were measured at the wall surface of the sinusoidal plate for different a / λ ratios, where, a is the amplitude and λ is the wavelength of the sinusoidal plate.

Yalamanchili [4-5], Sirivat and Rajagopal [4] did an experimental study which was very similar to the one which is being done currently. They studied the flow of non-Newtonian fluids with and without polymer additives in a corrugated channel using Laser Doppler Velocimetry. The centerline velocities and velocity profiles were studied for the flow of dilute polymer solutions, S. Muller [10].

A study of flow of non-Newtonian fluids through corrugated tubes was done by Phan-Thein and Khan [6], [11-12]. The tubes used were of small dimensions and Reynolds numbers studied were of the order of 10^{-4} .

2. KINEMATICS

The basic differential equations that represent the conservation of mass, momentum and energy of a system are formulated in this section. The basic definitions of kinematics and kinetics of bodies are described. For the purpose of deriving these equations the material is treated as a continuum.

2.1 Continuum Assumption

Assuming a material body to be a continuum means that there is sufficient number of molecules in the body of interest. We homogenize such a body and define field quantities over the homogeneous body which is referred to as the continuum associated with the body of interest.

If λ is the mean free path and L is the characteristic length or the length scale associated with the body then the Knudsen number K_n is defined as

$$K_n = \lambda / L \quad (2.1)$$

The Knudsen number is useful for determining whether continuum mechanics formulation of fluid dynamics should be used. If the K_n is close to or greater than 1 then the continuum assumption of fluid mechanics is not a good approximation (the mean free path of a molecule is comparable to a length scale). If $K_n \ll 1$ (0.01 or less) then we can say that our assumption of considering the body as a continuum is appropriate.

By treating the material as a continuum we are assuming the material to consist of an infinite number of material points. It is assumed that the manifold of material points is differentiable thus allowing the use of differential equations. The equations for motion of the material points are formulated with respect to one or more coordinate frames.

2.2 Kinematics

Let B represent an abstract body and $K_R(B)$ be some reference configuration of the fluid body. Let $K_t(B)$ denote the configuration of the body at time t . The motion of the body is referred to as χ (we assume the body is nicely differentiable). By motion of a body we mean a sufficiently smooth mapping which assigns to particles belonging to $K_R(B)$, particles belonging to $K_t(B)$.

$$\underline{x} = \chi(\underline{X}, t) \quad \text{or} \quad \underline{X} = \chi^{-1}(\underline{x}, t) \quad (2.2)$$

χ is the transformation that takes the body from X to x .

This is represented pictorially in figure 2.1.

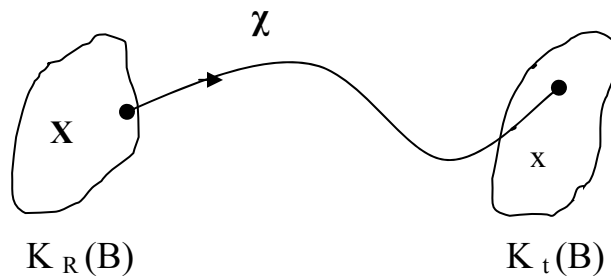


Figure 2.1. Motion of a Body

Any configuration can be chosen as the reference configuration hence the mapping itself changes with a change in the reference. If the reference configuration is the initial configuration the observation of motion is called Lagrangian motion and if the observation is made with respect to the current configuration then it is called as Eulerian motion.

A property ϕ (need not be a scalar) of a particle belonging to a body, at different instants of time can be expressed as,

$$\phi = \hat{\phi}(\underline{X}, t) = \tilde{\phi}(\underline{x}, t) \quad (2.3)$$

$\phi = \hat{\phi}(\underline{X}, t)$ is a Lagrangian specification while $\phi = \tilde{\phi}(\underline{x}, t)$ is a Eulerian specification.

The Eulerian approach describes changes as they occur at a fixed point in the fluid while the Lagrangian approach describes changes which occur as you follow a fluid particle along its trajectory. Generally in fluid mechanics an Eulerian approach is used.

The Displacement $\underline{u}(\underline{X}, t)$ is defined as,

$$\underline{u}(\underline{X}, t) = \underline{x} - \underline{X} = \chi(\underline{X}, t) - \underline{X} \quad (2.4)$$

The Velocity \underline{V} is defined as,

$$\underline{V} = \frac{d\underline{x}}{dt} \text{ or } \frac{d(\chi(\underline{X}, t))}{dt} \quad (2.5)$$

The deformation gradient \underline{F} is defined as,

$$\underline{F} = \frac{\partial \underline{x}}{\partial \underline{X}} \quad (2.6)$$

The velocity gradient \underline{L} is defined as,

$$\underline{L} = \frac{\partial \underline{V}}{\partial \underline{x}} \quad (2.7)$$

\underline{L} is written as $\text{grad } \underline{V}$ which is related to the deformation gradient as,

$$\underline{L} = \dot{\underline{F}}\underline{F}^{-1} \quad (2.8)$$

From equation 2.3, We also have the following possible derivatives.

The Lagrangian derivatives are given below:

$$\nabla\phi = \frac{\partial\hat{\phi}}{\partial\tilde{\mathbf{X}}}, \quad \frac{d\phi}{dt} = \frac{\partial\hat{\phi}}{\partial t} \quad (2.9)$$

The Eulerian derivatives are given below:

$$\text{grad}\phi = \frac{\partial\tilde{\phi}}{\partial\tilde{\mathbf{x}}}, \quad \frac{\partial\phi}{\partial t} = \frac{\partial\tilde{\phi}}{\partial t} \quad (2.10)$$

2.3 Balance Of Mass

2.3.1 Eulerian Approach

We consider a body B at a configuration $K_t(B)$ as shown in figure 2.2.

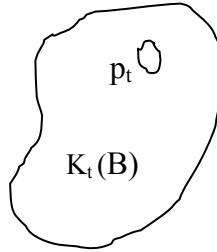


Figure 2.2. Body in the Current Configuration

$$\frac{\partial}{\partial t} \int_{p_t} \rho d\nu + \int_{\partial p_t} \rho \underline{\mathbf{V}} \cdot \underline{\mathbf{n}} = 0 \quad \forall p_t \subseteq K_t(B) \quad (2.11)$$

Where ρ is the density and $\underline{\mathbf{V}}$ is the velocity of the material

This can be reduced to,

$$\frac{\partial\rho}{\partial t} + \text{div}(\rho\underline{\mathbf{V}}) = 0 \quad (2.12)$$

Incompressibility condition results in the equation

$$\text{div}(\underline{\mathbf{V}}) = 0 \quad (2.13)$$

2.3.2 Lagrangian Approach

We consider the same body in the same configuration as in the Eulerian approach.

One form of equations for the balance of mass in Lagrangian approach is,

$$\rho_R = \rho_t \det \underline{F} \quad (2.14)$$

Where ρ_R and ρ_t are the densities in the reference and current configurations respectively.

Another form is,

$$\frac{d}{dt} \int_{P_t} \rho d\nu = 0 \quad (2.15)$$

2.4 Balance Of Linear Momentum

The balance of linear momentum can be written as

$$\text{div}(\underline{T}) + \rho \underline{b} = \rho \left(\frac{d \underline{V}}{dt} \right) = \rho \left(\frac{\partial \underline{V}}{\partial t} + (\nabla \underline{V}) \underline{V} \right) \quad (2.16)$$

Where, \underline{T} is the stress tensor also called the Cauchy stress tensor, ρ is the density of the body, \underline{b} represents the body forces and \underline{V} is the velocity vector.

In the absence of internal couples, the conservation of angular momentum reduces to the stress tensor being symmetric.

In equation form it can be written as,

$$\underline{T} = \underline{T}^T \quad (2.17)$$

2.5 Balance Of Energy

The balance of energy states that the change in the energy of a system is equal to the transfer of the energy to the system. This transfer of energy can occur in various forms

but restricting ourselves only to the mechanical and thermal forms of energy, the balance of energy can be written as:

$$\rho \dot{\varepsilon} + \text{div}(\mathbf{q}) = \mathbf{T} \cdot \mathbf{L} + \rho \mathbf{r} \quad (2.18)$$

Where, ε is the internal energy,

\mathbf{q} is the heat flux vector,

\mathbf{r} is the heat being radiated.

3. CONSTITUTIVE EQUATIONS

The model for a linearly viscous incompressible fluid is:

$$\underline{T} = -P\underline{I} + 2\mu\underline{D} \quad (3.1)$$

Where,

\underline{T} is the stress tensor

P is the hydrodynamic pressure

\underline{I} is identity

μ is the dynamic viscosity of the fluid

\underline{D} is the symmetric part of the velocity gradient

The fluid can undergo only isochoric motion. This results in the condition:

$$\text{tr}(\underline{D}) = 0 \quad (3.2)$$

For an incompressible fluid,

$$\det(\underline{F}) = 0 \quad (3.3)$$

This is the simplest condition for incompressibility because it directly relates to the material property. This leads to,

$$\text{div}(\underline{V}) = 0 \quad (3.4)$$

By substituting equations 3.2 and 3.3 in equation for balance of linear momentum we arrive at the Navier-Stokes equations which are the governing equations for an incompressible linearly viscous fluid. The Navier-Stokes equations in the general form are given by:

$$-\frac{\partial P}{\partial x_i} + \mu \Delta \underline{V} + \rho \underline{b} = \rho \frac{d \underline{V}}{d t} \quad (3.5)$$

Where, ρ is the density of the fluid, \underline{b} represents the body forces and \underline{V} is the velocity vector.

The type of fluid being discussed in this particular case is non-Newtonian, a shear-thinning fluid to be precise. The model used is a power law model which can be used to model shear-thinning fluids. The model is given by:

$$\underline{T} = -P \underline{I} + \mu_0 [1 + \alpha (\text{tr} \underline{D}^2)]^n \underline{D} \quad (3.6)$$

Where

μ_0 and α are the model parameters.

n is the power law index.

When the fluid is shear-thinning, n is less than 1, which means that its viscosity decreases with an increase in rate of shear. If the fluid is shear-thickening, n is greater than 1 and for a Newtonian fluid n is 0.

The term $\mu_0 [1 + \alpha (\text{tr} \underline{D}^2)]^n$ is called the generalized viscosity and can be represented by μ_e . This is a model for an incompressible generalized Stokesian fluid (it is capable of elastic response).

This model is used for doing all the simulations which are discussed in detail in the sections that follow.

The Governing equation is derived using this model. The stress tensor \underline{T} is evaluated and it is then substituted into the equation for balance of linear momentum. This gives us the governing equations for the model.

The governing equations are:

$$\begin{aligned} \rho \left(\frac{\partial u}{\partial t} + u \frac{\partial u}{\partial x} + v \frac{\partial u}{\partial y} + w \frac{\partial u}{\partial z} \right) = & -\frac{\partial P}{\partial x} + \alpha \frac{\mu_0}{2} n [K_1]^{n-1} \left[K_2 \frac{\partial u}{\partial x} + \frac{K_3}{2} \left(\frac{\partial u}{\partial y} + \frac{\partial v}{\partial x} \right) \right] \\ & + \alpha \frac{\mu_0}{2} n [K_1]^{n-1} \left[\frac{K_4}{2} \left(\frac{\partial u}{\partial z} + \frac{\partial w}{\partial x} \right) \right] \\ & + \frac{\mu_e}{2} \left[\frac{\partial^2 u}{\partial x^2} + \frac{\partial^2 u}{\partial y^2} + \frac{\partial^2 u}{\partial z^2} \right] + \rho b_x \end{aligned} \quad (3.7)$$

$$\begin{aligned} \rho \left(\frac{\partial v}{\partial t} + u \frac{\partial v}{\partial x} + v \frac{\partial v}{\partial y} + w \frac{\partial v}{\partial z} \right) = & -\frac{\partial P}{\partial y} + \alpha \frac{\mu_0}{2} n [K_1]^{n-1} \left[\frac{K_2}{2} \left(\frac{\partial u}{\partial y} + \frac{\partial v}{\partial x} \right) + K_3 \left(\frac{\partial v}{\partial y} \right) \right] \\ & + \alpha \frac{\mu_0}{2} n [K_1]^{n-1} \left[\frac{K_4}{2} \left(\frac{\partial v}{\partial z} + \frac{\partial w}{\partial y} \right) \right] \\ & + \frac{\mu_e}{2} \left[\frac{\partial^2 v}{\partial x^2} + \frac{\partial^2 v}{\partial y^2} + \frac{\partial^2 v}{\partial z^2} \right] + \rho b_y \end{aligned} \quad (3.8)$$

$$\begin{aligned} \rho \left(\frac{\partial w}{\partial t} + u \frac{\partial w}{\partial x} + v \frac{\partial w}{\partial y} + w \frac{\partial w}{\partial z} \right) = & -\frac{\partial P}{\partial z} + \alpha \frac{\mu_0}{2} n [K_1]^{n-1} \left[\frac{K_2}{2} \left(\frac{\partial w}{\partial x} + \frac{\partial u}{\partial z} \right) + \right] \\ & + \alpha \frac{\mu_0}{2} n [K_1]^{n-1} \left[\frac{K_3}{2} \left(\frac{\partial w}{\partial y} + \frac{\partial v}{\partial z} \right) + K_4 \left(\frac{\partial w}{\partial z} \right) \right] \\ & + \frac{\mu_e}{2} \left[\frac{\partial^2 w}{\partial x^2} + \frac{\partial^2 w}{\partial y^2} + \frac{\partial^2 w}{\partial z^2} \right] + \rho b_z \end{aligned} \quad (3.9)$$

Where K_1, K_2, K_3 and K_4 are given by,

$$K_1 = 1 + \alpha \left[\left(\frac{\partial u}{\partial x} \right)^2 + \left(\frac{\partial v}{\partial y} \right)^2 + \left(\frac{\partial w}{\partial z} \right)^2 + \frac{1}{2} \left(\frac{\partial u}{\partial y} + \frac{\partial v}{\partial x} \right)^2 + \frac{1}{2} \left(\frac{\partial u}{\partial z} + \frac{\partial w}{\partial x} \right)^2 \right] + \alpha \left[\frac{1}{2} \left(\frac{\partial w}{\partial y} + \frac{\partial v}{\partial z} \right)^2 \right] \quad (3.10)$$

$$K_2 = 2 \frac{\partial u}{\partial x} \left(\frac{\partial^2 u}{\partial x^2} \right) + 2 \frac{\partial v}{\partial y} \frac{\partial^2 v}{\partial x \partial y} + 2 \frac{\partial w}{\partial z} \left(\frac{\partial^2 w}{\partial x \partial z} \right) + \left(\frac{\partial u}{\partial y} + \frac{\partial v}{\partial x} \right) \left(\frac{\partial^2 u}{\partial x \partial y} + \frac{\partial^2 v}{\partial x^2} \right) + \left(\frac{\partial u}{\partial z} + \frac{\partial w}{\partial x} \right) \left(\frac{\partial^2 u}{\partial x \partial z} + \frac{\partial^2 w}{\partial x^2} \right) + \left(\frac{\partial w}{\partial y} + \frac{\partial v}{\partial z} \right) \left(\frac{\partial^2 w}{\partial x \partial y} + \frac{\partial^2 v}{\partial x \partial z} \right) \quad (3.11)$$

$$K_3 = 2 \frac{\partial u}{\partial x} \left(\frac{\partial^2 u}{\partial y \partial x} \right) + 2 \frac{\partial v}{\partial y} \frac{\partial^2 v}{\partial y^2} + 2 \frac{\partial w}{\partial z} \left(\frac{\partial^2 w}{\partial y \partial z} \right) + \left(\frac{\partial u}{\partial y} + \frac{\partial v}{\partial x} \right) \left(\frac{\partial^2 u}{\partial y^2} + \frac{\partial^2 v}{\partial y \partial x} \right) + \left(\frac{\partial u}{\partial z} + \frac{\partial w}{\partial x} \right) \left(\frac{\partial^2 u}{\partial y \partial z} + \frac{\partial^2 w}{\partial y \partial x} \right) + \left(\frac{\partial w}{\partial y} + \frac{\partial v}{\partial z} \right) \left(\frac{\partial^2 w}{\partial y^2} + \frac{\partial^2 v}{\partial y \partial z} \right) \quad (3.12)$$

$$K_4 = 2 \frac{\partial u}{\partial x} \left(\frac{\partial^2 u}{\partial z \partial x} \right) + 2 \frac{\partial v}{\partial y} \frac{\partial^2 v}{\partial z \partial y} + 2 \frac{\partial w}{\partial z} \left(\frac{\partial^2 w}{\partial z^2} \right) + \left(\frac{\partial u}{\partial y} + \frac{\partial v}{\partial x} \right) \left(\frac{\partial^2 u}{\partial z \partial y} + \frac{\partial^2 v}{\partial z \partial x} \right) + \left(\frac{\partial u}{\partial z} + \frac{\partial w}{\partial x} \right) \left(\frac{\partial^2 u}{\partial z^2} + \frac{\partial^2 w}{\partial z \partial x} \right) + \left(\frac{\partial w}{\partial y} + \frac{\partial v}{\partial z} \right) \left(\frac{\partial^2 w}{\partial z \partial y} + \frac{\partial^2 v}{\partial z^2} \right) \quad (3.13)$$

The Generalized viscosity,

$$\mu_e = \mu_0 [1 + \alpha (tr D^2)]^n \quad (3.14)$$

Equations (3.7) to (3.9) are the equations of motion which govern the fluid.

3.1 Non-Dimensionalization

- It is assumed that the flow is in a steady state. Hence the term $\frac{\partial \mathbf{V}}{\partial t}$ reduces to zero in the equation of motion.
- The body forces are also neglected. So the term $\rho \mathbf{b}$ is also zero.
- The equation of balance of mass and the equation of motion are non-dimensionalized by using appropriate non-dimensional quantities.
- A few assumptions made before doing this are that the fluid is assumed to be incompressible, the velocity in the direction of flow is assumed to be much greater than the velocity perpendicular to the flow ($u \gg v$), and the wavelength of the plate is assumed to be much greater than its amplitude ($\lambda \gg a$).
- $\tilde{x} = \frac{x}{\lambda}$, $\tilde{y} = \frac{y}{h}$, $\tilde{u} = \frac{u}{U}$, $\tilde{p} = \frac{p}{\rho U^2}$, $U = \frac{Q}{2bh}$ these were the non-dimensional quantities picked. The equations are then non-dimensionalized and an order of magnitude analysis is performed. Reynolds number was included in the equation.

4. PROBLEM DESCRIPTION AND PROCEDURE

The simulation of flow of a non-Newtonian fluid through corrugated channels is a very important problem from a research perspective. Its application can be found in various fields.

The idea is to simulate the flow of a shear-thinning fluid between a pair of corrugated plates. The plates have a sinusoidal profile. Four plates of varying amplitudes and wavelengths were modeled for the simulation. The length, breadth and height of the plates are kept constant.

The plate dimensions are mentioned in table 4.1.

Length (L) - 0.43 m

Breadth (b) - 0.089 m

Height (h) - 0.0073 m

Table 4.1. Plate Dimensions

Plate	Wavelength λ (m)	Amplitude a(m)
1	0.1016	0.0022
2	0.0254	0.0022
3	0.0254	0.0005
4	0.1016	0.0044

Shown in figure 4.1 is the front view of one of plates. All the geometric parameters are shown.

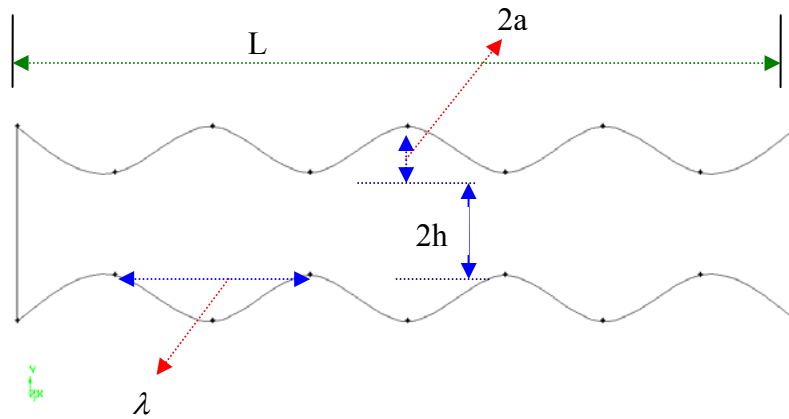


Figure 4.1. Schematic Diagram of a Plate

The simulations were done in two-dimensional space. A wide range of Reynolds numbers (Re) used for each plate. The Reynolds number used was a function of the half of the average plate spacing (h) and the velocity.

$$\text{Re} = \frac{U * h}{\nu} \quad (4.1)$$

Where,

Re is the Reynolds number

U is the velocity of the fluid

h is half the spacing between the plates

ν is the kinematic viscosity of the fluid

The kinematic viscosity ν is given by $\frac{\mu}{\rho}$ where μ is the dynamic viscosity and ρ is the density of the fluid.

The problem was also studied with the plate alignment being varied. The plates were positioned in three different ways with the first one being the crest of one plate being in phase with the crest of the second plate as shown in the figure below. In the second and

third positions the crest of one plate is 45° and 90° degrees out of phase with each other as shown in the figure 4.2, figure 4.3 and figure 4.4.

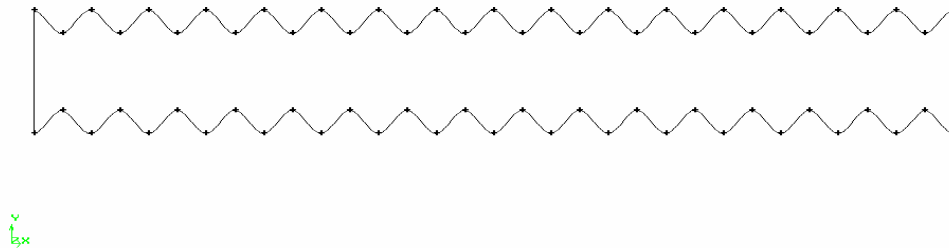


Figure 4.2. Plates Aligned with Each Other Without Any Phase Difference

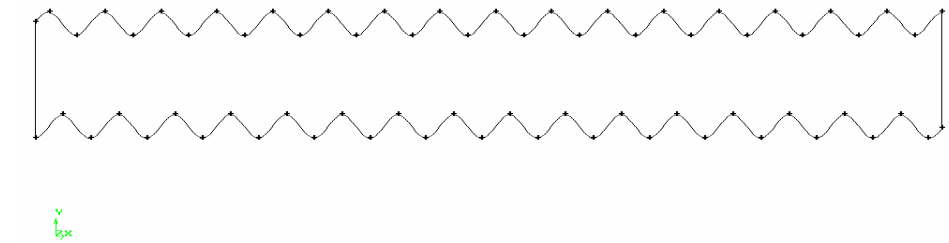


Figure 4.3. Plates Aligned with a Phase Difference of 45°

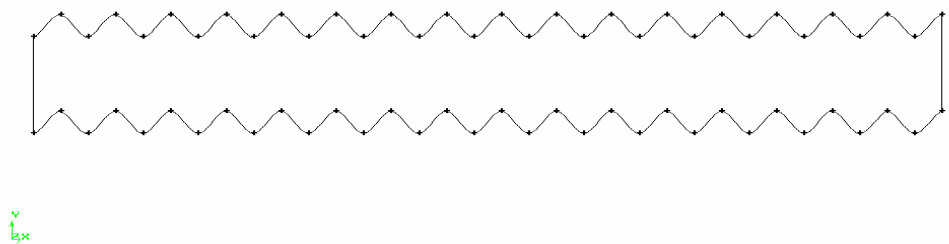


Figure 4.4. Plates Aligned with a Phase Difference of 90°

The measurements of the properties (velocity is the most important for this study) were made creating two additional lines called a crest line and a trough line. The crest line is defined as the line joining the points with maximum distance between the plates along the line and the trough is defined as the line joining the points with minimum distance between the plates along the line. The crest line and trough line are shown in the figure 4.5.

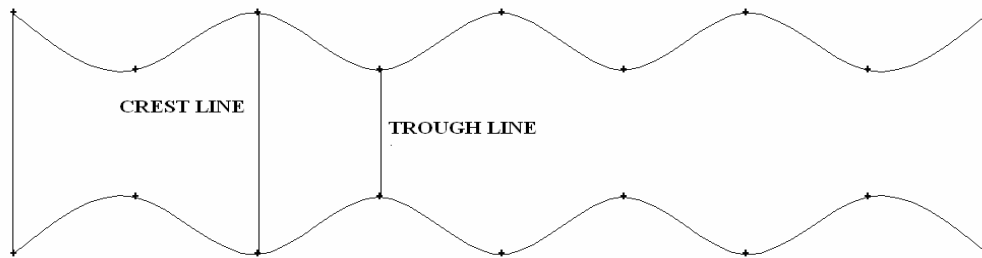


Figure 4.5. Schematic Diagram Showing the Crest Line and the Trough Line

4.1 Procedure For Numerical Simulation

The numerical simulation process starts with creating the geometry. This was done using GAMBIT version 2.3.16. The sinusoidal plates were generated using a line tool in GAMBIT used for generating NURBS (Non-Uniform Rational Basis-Spline).

The next step is to mesh the geometry. A structured mesh which is easy was used since the geometry was not too complex. All the elements used were quadrilateral for a two-dimensional geometry and hexadron for a three-dimensional one. The grid spacing used was 0.01. The zone types were set in GAMBIT. The zone types used were wall, mass flow inlet and pressure outlet. The boundaries and zone types for a typical case are shown in the figure 4.6.

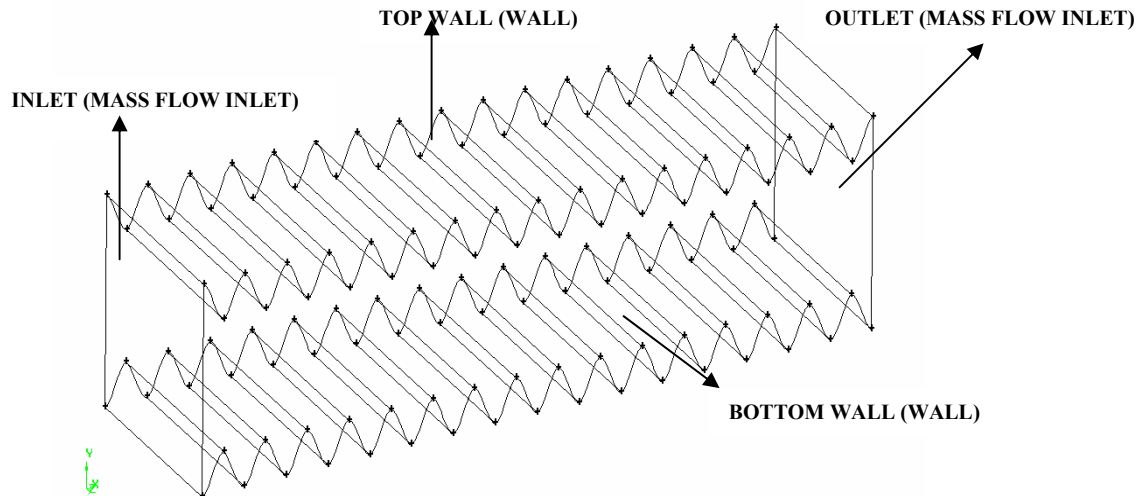


Figure 4.6. Boundary and Zone Types

The figure below shows the mesh for one of the cases. The figure shown is of plate 4 with amplitude of 0.1016 m and a wavelength of 0.0044 m. The mesh used for all the cases have quadrilateral elements with a very fine grid spacing of 0.05. The mesh shown in figure 4.7 has about 50,000 elements.

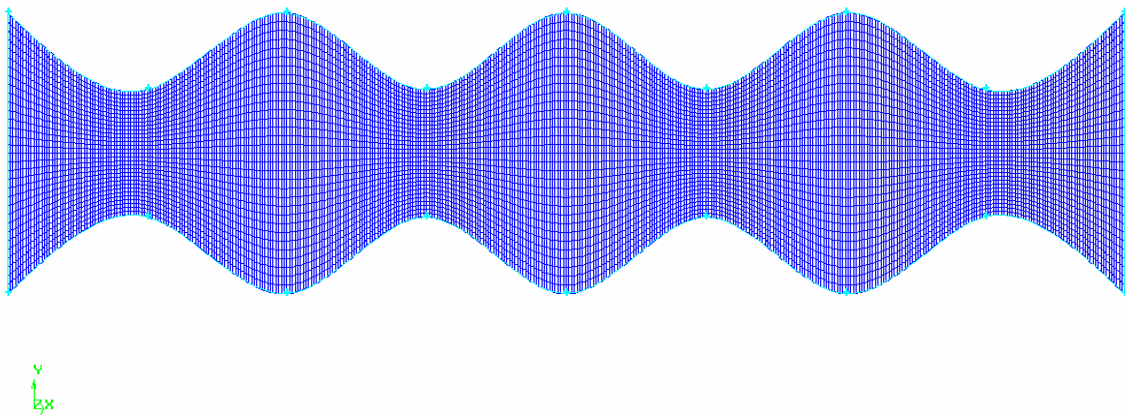


Figure 4.7. Two-Dimensional Mesh

Following the designation of the zone types, the meshed geometry is then exported as a mesh file and then imported into FLUENT. FLUENT version 6.3.26 was used. The following procedure was followed while using Fluent.

- The mesh is checked for irregularities using a grid check to make sure it is ready to be used. The grid is scaled to be used in centimeters. This is done for convenience. The results are presented in SI units.
- The units for various parameters such as length, pressure, velocity, mass flow rate and temperature are set to SI units.
- The model to be used for solving the problem is written as a C program. This program is imported as an interpreted user defined function and compiled. Now it is ready to be used.
- The material to be used is defined. Oil and blood were used as fluids. Oil is a predefined material in the FLUENT database, while blood had to be defined by the user by creating a new material. The properties of the fluids are shown in table 4.2. The viscosity is user-defined. In the drop-down menu next to the viscosity the option for viscosity to be “user defined” is chosen. Thereby, the model to be used for the viscosity which was compiled in the previous step is input and this is used to calculate the changes in viscosity since the viscosity is not a constant for the fluid being used.

Table 4.2. Material Properties

PROPERTY	BLOOD	OIL
Density, $\rho \left(\frac{\text{kg}}{\text{m}^3} \right)$	1060	960
Specific heat, $C_p \left(\frac{\text{J}}{\text{kg.k}} \right)$	3594	1880
Thermal conductivity, $K \left(\frac{\text{W}}{\text{m.k}} \right)$	0.00152	0.12
Dynamic Viscosity, $\mu \left(\frac{\text{kg}}{\text{m.s}} \right)$	0.0035	0.048

- The boundary conditions are then defined. The mass flow rate (\dot{m}) is calculated and defined using the area of the inlet section and the velocity to be used. The velocity to be used is calculated previously using the relation for Reynolds number.
- Since h and ν are constants for all the cases and some of the other parameters like the length of the plate (L) and its breadth (b) are also constants, the values used for the velocity are non-dimensional. The non-dimensionalization was carried out as explained in section 3.1. The other boundary condition that needs to be defined is the pressure outlet.
- The solver used is a density based solver which was discussed previously in this section and the flow is assumed to be laminar. The Reynolds number is varied from 100 to 1000. The Reynolds numbers for the data presented in the results are 100, 500 and 1000.
- There were four plates that were modeled and each plate was modified in three ways with phase difference of 0° , 45° and 90° between top and the bottom plates. Each of these 12 cases was simulated for three different Reynolds numbers which are 100, 500 and 1000. So a total of 36 cases were simulated in all.
- The solution was monitored and residuals were plotted after every iteration and the difference in mass flow rate between the inlet and outlet was also plotted.
- The solution was allowed to continue to run till the value of mass flow rate at the pressure outlet had reached a value very close to the one specified at the inlet.
- Then the post processing was done, a process which includes collecting the data required, sorting it, analyzing it and making modifications.

5. NUMERICAL SIMULATION

5.1 Fluent

Fluent is a computer program for modeling fluid flow and heat transfer. It is written using the computer language C and takes advantage of the power and flexibility offered by the C. Consequently, true dynamic memory allocation, efficient data structures, and flexible solver control are all possible. It provides mesh flexibility and allows for problems to be solved using both structured and unstructured meshes. Triangular and quadrilateral are the supported mesh types in 2D while in 3D they are tetrahedral, hexahedral, pyramid, wedge, polyhedral, and mixed (hybrid) meshes. FLUENT also allows for the mesh to be refined or coarsened, based on the flow situation. If we need more accuracy in a particular region we refine the mesh and if there is a region where we do not need much accuracy or is not critical to the flow field we coarsen the mesh to save computational time. FLUENT used a client/server architecture which allows for efficient execution, interactive control, and complete flexibility between different types of machines or operating systems. All functions required to compute a solution and display the results are accessible in Fluent through an interactive, menu-driven interface.

The Fluent package consists of Fluent, the solver, Gambit, the preprocessor that is used for the geometry modeling and mesh generation, an additional preprocessor that can generate volume meshes from boundary meshes and finally some filters which are capable of importing surface and volume meshes from other CAD/CAE packages.

The figure 5.1 shows the general structure of Fluent program.

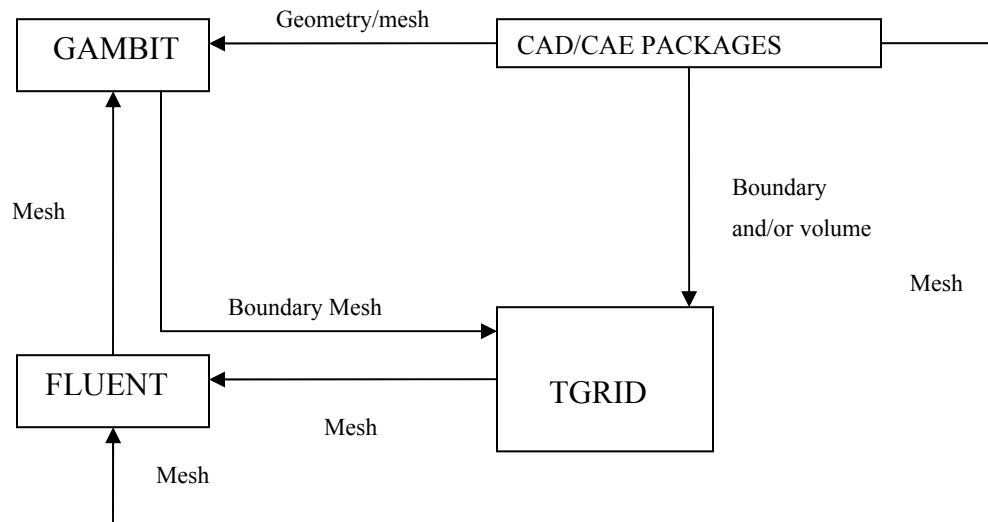


Figure 5.1. Structure of Fluent Program

5.2 Running Fluent And Gambit

FLUENT and GAMBIT were run remotely on a Texas A&M University supercomputer during the entire analysis process. A program called X-WIN32 which allows us to remotely connect to the supercomputer was used. X-WIN32 acts as an interface to communicate with the supercomputer. It also provides a graphical interface that helps in displaying the graphics on the screen. Three supercomputers that are capable of running FLUENT and GAMBIT were available namely AGAVE, COSMOS and K2. Another program called WINSCP382 was used to manage the files. Files can be transferred from and to the supercomputers using WINSCP382.

5.3 Gambit

GAMBIT is a software package designed to help in building mesh models for computational fluid dynamics (CFD). GAMBIT receives user input by means of its graphical user interface (GUI). The GAMBIT GUI makes the basic steps of building, meshing, and assigning zone types to a model simple and intuitive, yet it is versatile enough to accommodate a wide range of modeling applications.

The three steps of creating and meshing a geometry using GAMBIT is as follows:

- Creating the geometry
- Meshing the geometry
- Assigning appropriate zone to the boundaries

5.4 Geometry

A critical part of creating the geometry is generation of the corrugated plates. These plates have a sinusoidal contour with different plates having different wavelengths and amplitude. These plates were generated using a line tool in Gambit used for generating NURBS (Non-Uniform Rational Basis-Spline). NURBS is a mathematical model commonly used in computer graphics for generating and representing curves and surfaces. This tool needs the points on the sinusoidal curve to be specified.

Gambit provides two methods for constructing a NURBS edge.

- Interpolate
- Approximate

In the Interpolate method the edge to passes through all specified vertices while the approximate method creates an edge that passes near to all interior vertices to within a specified tolerance. In both cases, the new edge begins and ends at the first and last specified vertices.

5.5 Meshing

Gambit allows the use of structured and unstructured mesh to mesh the geometry. A combination of the two can also be used. This is done by splitting the geometry into several zones and meshing the zones individually. A structured mesh

Gambit incorporates a wide variety of meshing techniques. There are options to mesh the following entities.

- Edge
- Face
- Volume
- Group

The Mesh Edges command allows you to grade or mesh any or all edges in the model. When you grade an edge, Gambit applies the mesh node spacing specifications but does not create mesh nodes on the edge. When you mesh an edge, Gambit creates mesh nodes according to the specifications.

The Mesh Faces command allows you to create the mesh for one or more faces in the model. When you mesh a face, Gambit creates mesh nodes on the face according to the currently specified meshing parameters.

The Mesh Volumes command allows you to create a mesh for one or more volumes in the model. When you mesh a volume, Gambit creates mesh nodes throughout the volume according to the currently specified meshing parameters.

To mesh a volume, you must specify the following parameters:

- entity to be meshed
- Meshing scheme
- Mesh node spacing
- Meshing options

The Mesh Groups command activates meshing operations for one or more groups of topological entities.

When you mesh a group by means of the Mesh Groups command, Gambit performs meshing operations for all of the topological entities that comprise components of the group. If you apply meshing parameters to any or all components of the group prior to executing the Mesh Groups command, Gambit meshes those components according to

their previously applied parameters. All other components of the group are meshed according to the default meshing parameters. For example, if you mesh a group that includes three edges to one of which has been previously applied a double-sided, successive-ratio grading scheme, Gambit honors the applied scheme when it meshes the group but meshes the other two edges according to the current default grading scheme.

To perform a group meshing operation, you must specify the following parameters:

- Group name(s)
- Mesh node spacing

5.5.1 Specifying Zone Type

The next step after meshing is to specify zone types to the various boundaries. Zone-type specifications define the physical and operational characteristics of the model at its boundaries and within specific regions of its domain. There are two classes of zone-type specifications:

- Boundary types
- Continuum types

Boundary-type specifications, such as wall or pressure outlet define the characteristics of the model at its external or internal boundaries. Continuum-type specifications, such as fluid or solid, define the characteristics of the model within specified regions of its domain.

Some of the available zone types are inflow, inlet, inlet vent, interior, internal, mass flow inlet, membrane, moving boundary, node outflow, outlet, outlet vent, periodic, porous, pressure, pressure far field, pressure inflow, pressure inlet, pressure outflow, pressure outlet, radiation, radiator, recirculation inlet, recirculation outlet, surface, symmetry, traction, velocity, velocity inlet and vent wall.

5.5.2 Boundary Layers

Boundary layers define the spacing of mesh node rows in regions immediately adjacent to edges and/or faces. They are used primarily to control mesh density and, thereby, to control the amount of information available from the computational model in specific regions of interest.

As an example of a boundary layer application, consider a computational model that includes a cylinder representing a pipe through which flows a viscous fluid. Under normal circumstances, it is likely that the fluid velocity gradients are large in the region immediately adjacent to the pipe wall and small near the center of the pipe. By attaching a boundary layer to the face that represents the pipe wall, you can increase the mesh density near the wall and decrease the density near the center of the cylinder, thereby obtaining sufficient information to characterize the gradients in both regions while minimizing the total number of mesh nodes in the model.

To define a boundary layer, you must specify the following information:

- Boundary-layer algorithm
- Height of the first row of mesh elements
- Growth factor—which specifies the height of each succeeding row of elements
- Total number of rows—which defines the depth of the boundary layer
- Edge or face to which the boundary layer is attached
- Face or volume that defines the direction of the boundary layer

5.6 The Fluent Process

Once a mesh has been read into FLUENT, all remaining operations are performed within FLUENT. These include setting boundary conditions, defining fluid properties, executing the solution, refining the mesh, and viewing and post processing the results. The mesh generated using GAMBIT or some other mesh generating technique is imported into

FLUENT. The mesh which was generated using GAMBIT in this case contains the geometry and the mesh. The boundaries are also assigned specific zone types.

The FLUENT serial solver manages file input and output, data storage, and flow field calculations using a single solver process on a single computer. FLUENT also uses a utility called cortex that manages FLUENT's user interface and basic graphical functions. FLUENT's parallel solver allows you to compute a solution using multiple processes that may be executing on the same computer, or on different computers in a network.

5.7 Steps In Solving A CFD Problem

Once you have determined the important features of the problem you want to solve, follow the basic procedural steps shown below.

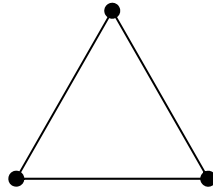
1. Define the modeling goals.
2. Create the model geometry and grid.
3. Set up the solver and physical models.
4. Compute and monitor the solution.
5. Examine and save the results.
6. Consider revisions to the numerical or physical model parameters, if necessary.

Fluent being an unstructured solver uses internal data structures to assign an order to the cells, faces, and grid points in a mesh and to maintain contact between adjacent cells. Therefore, it does not require i, j, k indexing to locate neighboring cells. This gives you the flexibility to use the best grid topology for your problem, as the solver does not force an overall structure or topology on the grid.

In 2D, quadrilateral and triangular cells are accepted, and in 3D, hexahedral, tetrahedral, pyramid, wedge, and polyhedral cells can be used. These cells are shown in figure 5.2. Both single-block and multi-block structured meshes, as well as hybrid meshes containing quadrilateral and triangular cells or hexahedral, tetrahedral, pyramid, and wedge cells are acceptable. Fluent also accepts grids with hanging nodes (i.e., nodes on edges and faces that are not vertices of all the cells sharing those edges or faces). Grids

with non-conformal boundaries (i.e., grids with multiple sub-domains in which the grid node locations at the internal sub-domain boundaries are not identical) are also acceptable.

2D Cells

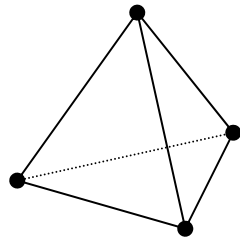


Triangle

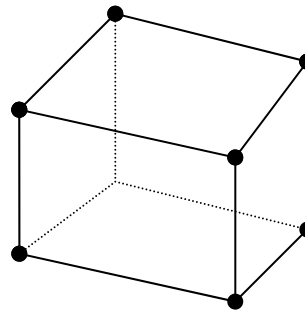


Quadrilateral

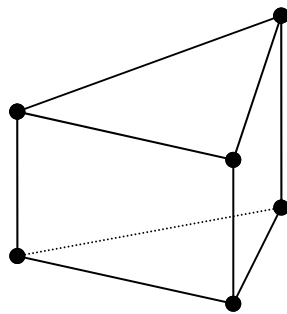
3D Cells



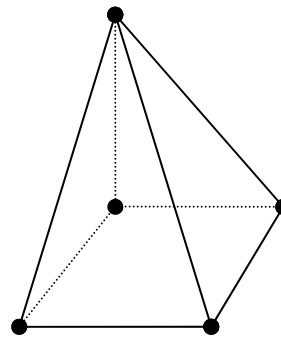
Tetrahedron



Hexahedron



Prism/Wedge



Pyramid

Figure 5.2. Types of Elements Used in Gambit

5.8 Setting Boundary Types

The boundary types available in FLUENT are classified as follows:

- Flow inlet and exit boundaries: pressure inlet, velocity inlet, mass flow inlet, and inlet vent, intake fan, pressure outlet, pressure far-field, outflow, outlet vent, and exhaust fan.
- Wall, repeating, and pole boundaries: wall, symmetry, periodic, and axis.
- Internal cell zones: fluid, and solid (porous is a type of fluid zone).

Internal face boundaries: fan, radiator, porous jump, wall, and interior

Of these boundary types the one which was used extensively for the current model are wall, mass flow inlet and pressure outlet.

5.8.1 Mass Flow Boundary Condition

Mass flow boundary conditions can be used in FLUENT to provide a prescribed mass flow rate or mass flux distribution at an inlet. Physically, specifying the mass flux permits the total pressure to vary in response to the interior solution. This is in contrast to the pressure inlet boundary condition, where the total pressure is fixed while the mass flux varies.

A mass flow inlet is often used when it is more important to match a prescribed mass flow rate than to match the total pressure of the inflow stream. An example is the case of a small cooling jet that is bled into the main flow at a fixed mass flow rate, while the velocity of the main flow is governed primarily by a (different) pressure inlet/outlet boundary condition pair.

You will enter the following information for a mass flow inlet boundary:

- mass flow rate, mass flux, or (primarily for the mixing plane model) mass flux with average mass flux
- total (stagnation) temperature
- static pressure
- flow direction

When mass flow boundary conditions are used for an inlet zone, a velocity is computed for each face in that zone, and this velocity is used to compute the fluxes of all relevant solution variables into the domain. With each iteration, the computed velocity is adjusted so that the correct mass flow value is maintained.

To compute this velocity, your inputs for mass flow rate, flow direction, static pressure, and total temperature are used.

There are two ways to specify the mass flow rate. The first is to specify the total mass flow rate, m , for the inlet. The second is to specify the mass flux, ρv_n (mass flow rate per unit area). If a total mass flow rate is specified, FLUENT converts it internally to a uniform mass flux by dividing the mass flow rate by the total inlet area:

$$\rho v_n = \frac{m}{A} \quad (5.1)$$

If the direct mass flux specification option is used, the mass flux can be varied over the boundary by using profile files or user-defined functions. If the average mass flux is also specified (either explicitly by you or automatically by FLUENT), it is used to correct the specified mass flux profile, as described earlier in this section.

Once the value of ρv_n at a given face has been determined, the density, ρ , at the face must be determined in order to find the normal velocity (v_n). The manner in which the density is obtained depends upon whether the fluid is modeled as an ideal gas or not. Each of these cases is examined below.

5.8.2 Wall Boundary Conditions

Wall boundary conditions are used to bound fluid and solid regions. In viscous flows, the no-slip boundary condition is enforced at walls by default, but you can specify a tangential velocity component in terms of the translational or rotational motion of the wall boundary, or model a "slip" wall by specifying shear. (You can also model a slip

wall with zero shear using the symmetry boundary type, but using a symmetry boundary will apply symmetry conditions for all equations.)

The shear stress and heat transfer between the fluid and wall are computed based on the flow details in the local flow field.

5.9 Shear-Stress Calculation At Wall Boundaries

For no-slip wall conditions, FLUENT uses the properties of the flow adjacent to the wall/fluid boundary to predict the shear stress on the fluid at the wall. In laminar flows this calculation simply depends on the velocity gradient at the wall.

For specified-shear walls, FLUENT will compute the tangential velocity at the boundary.

If you are modeling inviscid flow with FLUENT, all walls use a slip condition, so they are frictionless and exert no shear stress on the adjacent fluid.

5.10 Shear-Stress Calculation In Laminar Flow

In a laminar flow, the wall shear stress is defined by the normal velocity gradient at the wall as

$$\tau_w = \mu \left(\frac{\partial v}{\partial n} \right) \quad (5.2)$$

When there is a steep velocity gradient at the wall, you must be sure that the grid is sufficiently fine to accurately resolve the boundary layer.

5.11 Defining Materials

An important step in the setup of the model is to define the materials and their physical properties. Material properties are defined in the Materials panel, where you can enter values for the properties that are relevant to the problem scope you have defined in the Models panel. These properties may include the following:

- density and/or molecular weights
- viscosity
- heat capacity
- thermal conductivity
- UDS diffusion coefficients
- mass diffusion coefficients
- standard state enthalpies
- kinetic theory parameters

Properties may be temperature-dependent and/or composition-dependent, with temperature dependence based on a polynomial, piecewise-linear, or piecewise-polynomial function and individual component properties either defined by you or computed via kinetic theory.

5.12 Material Types And Databases

In FLUENT, you can define six types of materials: fluids, solids, mixtures, combusting-particles, droplet-particles, and inert-particles. Physical properties of fluids and solids are associated with named materials. These materials are then assigned as boundary conditions for zones.

5.13 Viscosity

Fluent provides several options for definition of the fluid viscosity:

- constant viscosity
- temperature dependent and/or composition dependent viscosity
- kinetic theory
- non-Newtonian viscosity
- user-defined function

Fluent provides four options for modeling non-Newtonian flows:

- power law

- Carreau model for pseudo-plastics
- Cross model
- User-defined viscosity

A user-defined function was used for the viscosity

5.14 The Solver

Fluent allows you to choose one of the two numerical methods:

- pressure-based solver
- density-based solver

The pressure-based approach was developed for low-speed incompressible flows, while the density-based approach is mainly used for high-speed compressible flows. However, recently both methods have been extended and reformulated to solve and operate for a wide range of flow conditions beyond their traditional or original intent.

In both methods the velocity field is obtained from the momentum equations. In the density-based approach, the continuity equation is used to obtain the density field while the pressure field is determined from the equation of state.

On the other hand, in the pressure-based approach, the pressure field is extracted by solving a pressure equation or pressure correction equation which is obtained by manipulating continuity and momentum equations.

Using either method, Fluent will solve the governing integral equations for the conservation of mass and momentum, and (when appropriate) for energy and other scalars such as turbulence and chemical species. In both cases a control-volume-based technique is used that consists of:

- Division of the domain into discrete control volumes using a computational grid.

- Integration of the governing equations on the individual control volumes to construct algebraic equations for the discrete dependent variables ("unknowns") such as velocities, pressure, temperature, and conserved scalars.
- Linearization of the discretized equations and solution of the resultant linear equation system to yield updated values of the dependent variables.

The two numerical methods employ a similar discretization process (finite-volume), but the approach used to linearize and solve the discretized equations is different.

The density-based solver solves the governing equations of continuity, momentum, and (where appropriate) energy and species transport simultaneously (i.e., coupled together). Governing equations for additional scalars will be solved afterward and sequentially (i.e., segregated from one another and from the coupled set) using the procedure described below. Because the governing equations are non-linear (and coupled), several iterations of the solution loop must be performed before a converged solution is obtained.

- Update the fluid properties based on the current solution. (If the calculation has just begun, the fluid properties will be updated based on the initialized solution.)
- Solve the continuity, momentum, and (where appropriate) energy and species equations simultaneously.
- Where appropriate, solve equations for scalars such as turbulence and radiation using the previously updated values of the other variables.
- When interphase coupling is to be included, update the source terms in the appropriate continuous phase equations with a discrete phase trajectory calculation.
- Check for convergence of the equation set.

These steps are continued until the convergence criteria are met.

In the density-based solution method you can solve the coupled system of equations (continuity, momentum, energy and species equations if available) using, either the

coupled-explicit formulation or the coupled-implicit formulation. The main distinction between the density-based explicit and implicit formulations is described next.

In the density-based solution methods the discrete, non-linear governing equations are linearized to produce a system of equations for the dependent variables in every computational cell. The resultant linear system is then solved to yield an updated flow-field solution.

The manner in which the governing equations are linearized may take an "implicit" or "explicit" form with respect to the dependent variable (or set of variables) of interest. By implicit or explicit we mean the following:

- Implicit: For a given variable, the unknown value in each cell is computed using a relation that includes both existing and unknown values from neighboring cells. Therefore each unknown value will appear in more than one equation in the system, and these equations must be solved simultaneously to give the unknown quantities.
- Explicit: For a given variable, the unknown value in each cell is computed using a relation that includes only existing values. Therefore each unknown will appear in only one equation in the system and the equations for the unknown value in each cell can be solved one at a time to give the unknown quantities.

5.15 User Defined Functions

A user-defined function, or UDF, is a function that you program, that can be dynamically loaded with the FLUENT solver to enhance the standard features of the code. For example, you can use a UDF to define your own boundary conditions, material properties, and source terms for your flow regime, as well as specify customized model parameters (e.g., DPM, multiphase models), initialize a solution, or enhance post-processing.

UDFs are written in the C programming language using any text editor and the source code file is saved with a .c extension. One source file can contain a single UDF or multiple UDFs, and you can define multiple source files.

UDFs are defined using DEFINE macros provided by Fluent Inc. They are coded using additional macros and functions that access Fluent solver data and perform other tasks.

Every UDF must contain the udf.h file inclusion directive (`#include "udf.h"`) at the beginning of the source code file, which allows definitions of DEFINE macros and other Fluent-provided macros and functions to be included during the compilation process. Note that values that are passed to a solver by a UDF or returned by the solver to a UDF are specified in SI units.

Source files containing UDFs can be either interpreted or compiled in Fluent. For interpreted UDFs, source files are interpreted and loaded directly at runtime, in a single-step process. An interpreted UDF was used in this case. For compiled UDFs, the process involves two separate steps. A shared object code library is first built and then it is loaded into FLUENT. Once interpreted or compiled, UDFs will become visible and selectable in Fluent graphics panels, and can be hooked to a solver by choosing the function name in the appropriate panel.

In summary, UDFs:

- Are written in the C programming language.
- Must have an include statement for the udf.h file.
- Must be defined using DEFINE macros supplied by Fluent Inc.
- Utilize predefined macros and functions supplied by Fluent Inc. to access Fluent solver data and perform other tasks.
- Are executed as interpreted or compiled functions.
- Are hooked to a Fluent solver using a graphical user interface panel.
- Use and return values specified in SI units.

The program which was written in C is:

```
# include "udf.h"
# define n 0.67
# define alpha 1.0
# define muo 0.0042
DEFINE_PROPERTY(Power_law_model,cell,thread)
{
    float visc,trace;
    float u[3],v[3],w[3];
    int i;
    for(i=0; i<3; i++)
    {
        u[i] = C_U_G(cell,thread)[i];
        v[i] = C_V_G(cell,thread)[i];
        w[i] = C_W_G(cell,thread)[i];
    }
    trace = 0.5*(2*pow(u[0],2) + pow(v[0]+u[1],2) + 2*pow(v[1],2) +
        pow(v[2]+w[1],2) + 2*pow(w[2],2) + pow(w[0]+u[2],2));
    visc = 0.5*muo*pow(1+alpha*trace,0.67);
    return visc;
}
```

6. RESULTS AND CONCLUSIONS

After the solution had converged the next step in the process is post processing. This consisted of setting up the solution such that the data we need from the solution can be extracted. The data acquired from each case consisted of:

- The velocity profiles at the center line, crest line and trough line.
- Images of the velocity contours showing the distribution of velocity between the plates.
- Images of the velocity vectors in the regions where there are recirculation zones.
- The distribution of wall shear stress along the top wall.

Since there are 36 cases and a lot of data, it is not possible to include all the data in this report. Hence only the important results are included in this section.

6.1 Plate 1

The velocity contours of the plate 1 are shown in figure 6.1. The fluid used is blood. The phase angle between the plates is 0° .

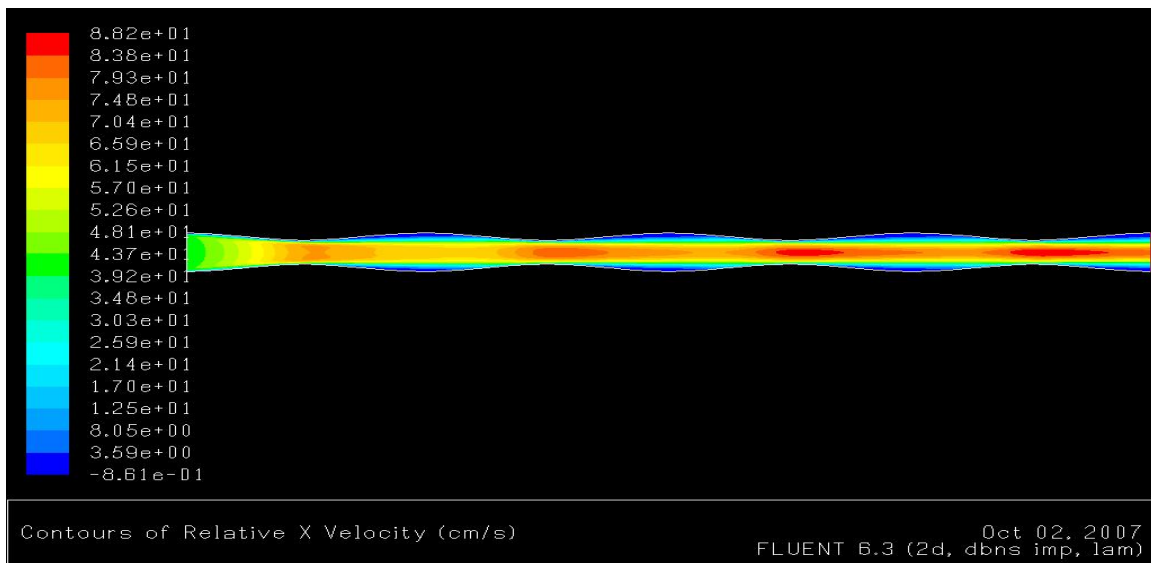


Figure 6.1. Velocity Contours, Blood, $a = 0.0022$, $\lambda = 0.1016$, $Re = 1000$

The inlet velocity is 0.412 m/s. This region is colored in green. From there the flow accelerated when the cross-section area decreases, and slows down when the cross-section area increases. The flow accelerates to a maximum velocity of 0.882 m/s which is twice the value at the inlet. The centerline velocity along the length of the plate can be seen in the figure below.

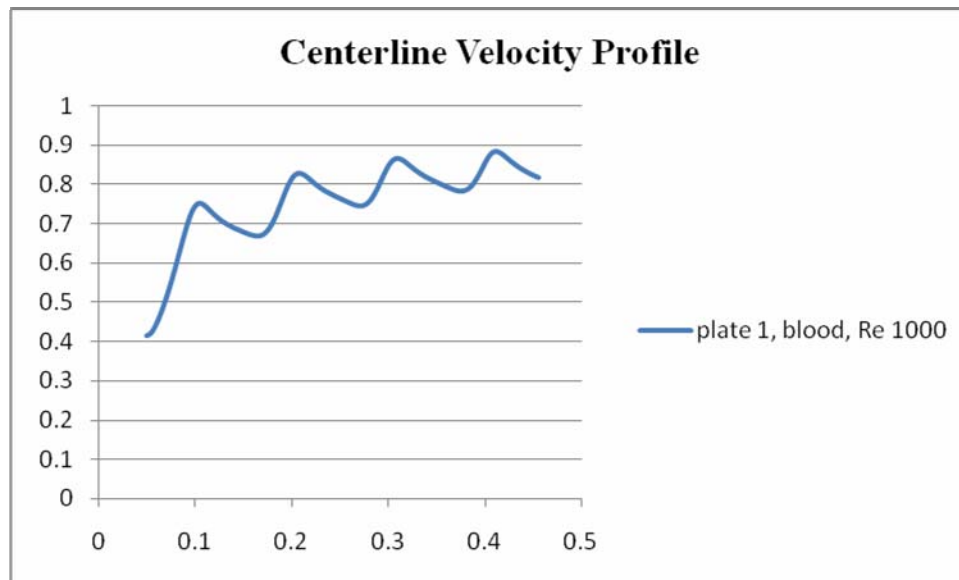


Figure 6.2. Plate 1, Centerline Velocity Profile, Blood

It can be seen that the velocity flow keeps accelerating all the way till the end except for when there is increase in the cross section area. There are recirculation zones in this case but they are not clearly visible because of their very low velocity which has a magnitude of 0.0155 m/s in the opposite direction of the flow.

A similar pattern is observed in the velocity contour for the case in which oil is used as the fluid. The same Reynolds number (1000) is used. The velocity in this case at the inlet is 6.84 m/s. The velocity vectors near the expansion region are shown below. It can be seen in the figure that there is a predominant recirculation region. The maximum value of velocity in this region is 9.13 m/s in the opposite direction of the flow. The flow accelerates to a maximum value of 14.8 m/s when is more than twice the value at the inlet.

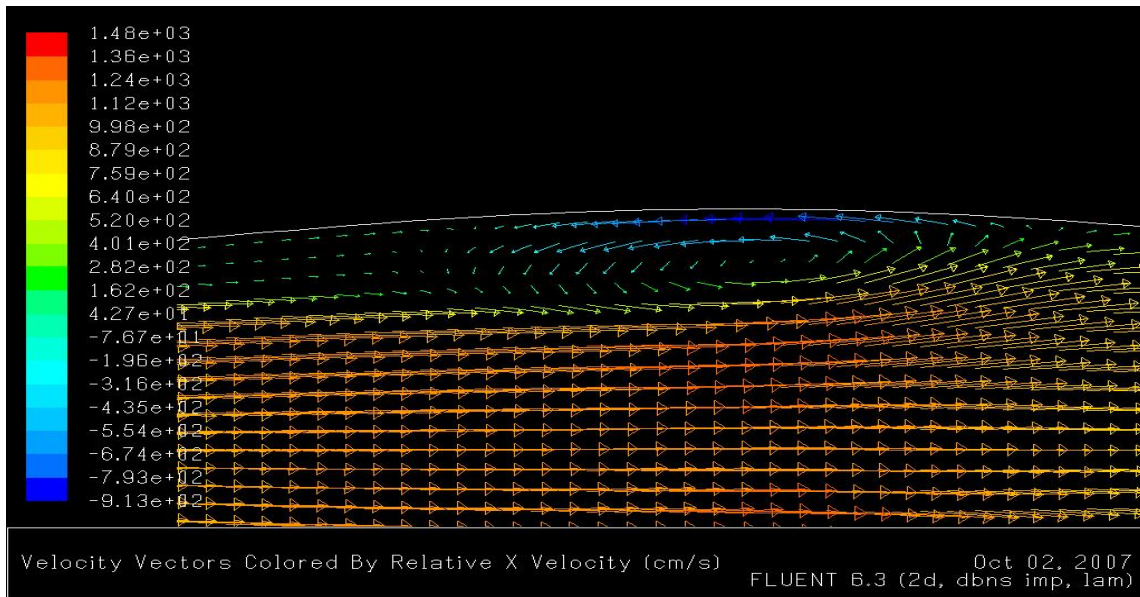


Figure 6.3. Plate 1 Velocity Vectors, Oil, $a = 0.0022$, $\lambda = 0.1016$, $Re = 1000$

Shown in figure 6.4 is the center line velocity plot for the same case.

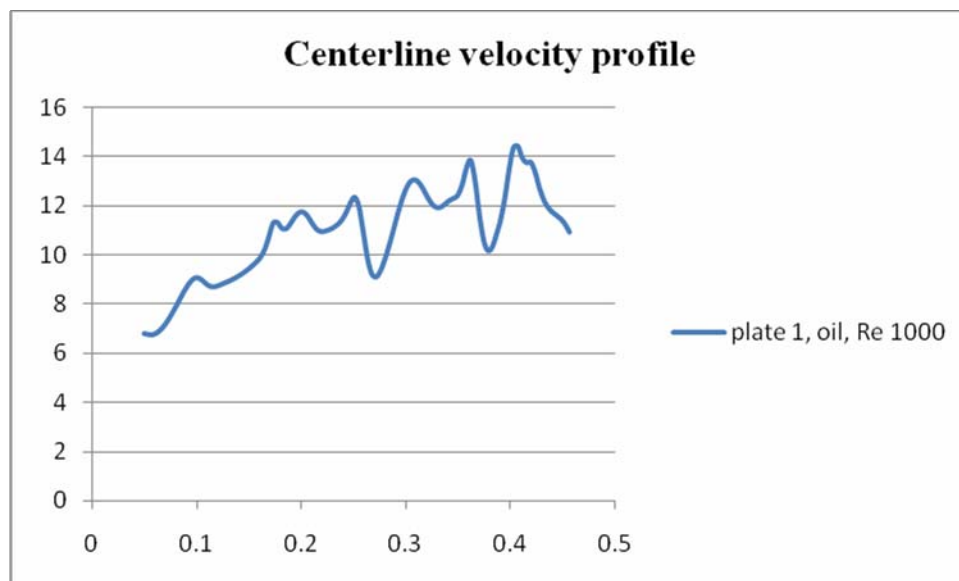


Figure 6.4. Plate 1, Oil, $Re = 1000$, Centerline Velocity Profile

Shown below is a velocity plot for the same case along the trough line. It can be seen that the flow changes direction as it approaches the plates. The maximum velocity in the opposite direction is a very large number too (9.13 m/s).

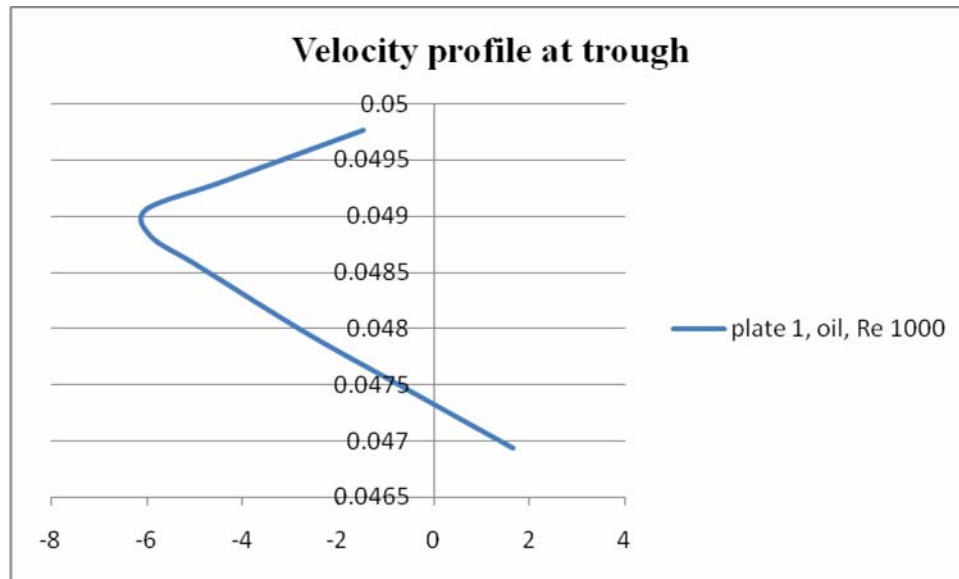


Figure 6.5. Velocity Profile at Trough Line, Oil, Re = 1000

Seen in figure 6.6 is the velocity plot along the trough line for a Reynolds number of 500. The reversed flow has a lower maximum velocity (1.5 m/s), when compared to the case with Reynolds number 1000 which is obvious but even the proportion of this velocity compared to the inlet velocity (3.42 m/s) is low. It is only half the inlet velocity. This shows that as the Reynolds number increases the effect reversed flow. The reversed flow seems to affect the maximum velocity of the flow. The more the reversed flow (the maximum velocity of the reversed flow) more the maximum velocity in proportion to the inlet velocity.

Shown in figure 6.7 are the velocity vectors for a similar case with oil as fluid and the Reynolds number of 100. The inlet velocity is 0.68 m/s. Reversed flow can still be observed even at such a low Reynolds number and inlet velocity. The flow is accelerated to a maximum velocity of 1.42 m/s.

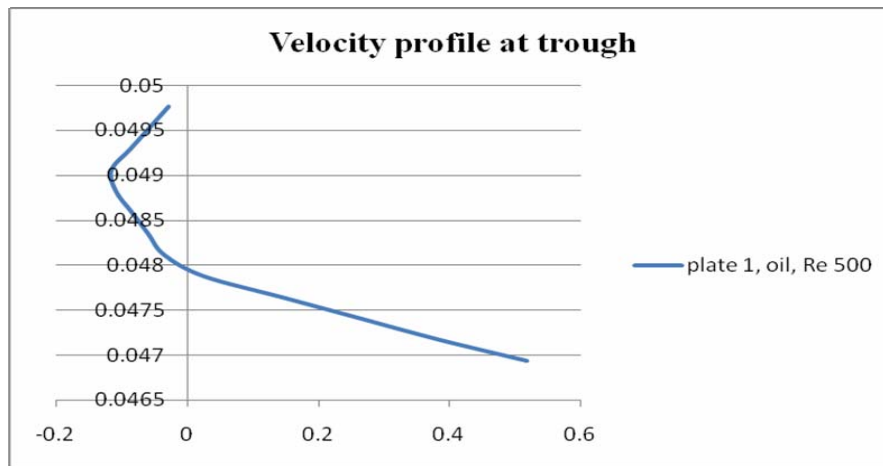


Figure 6.6. Velocity Profile at Trough Line, Oil, Re = 500

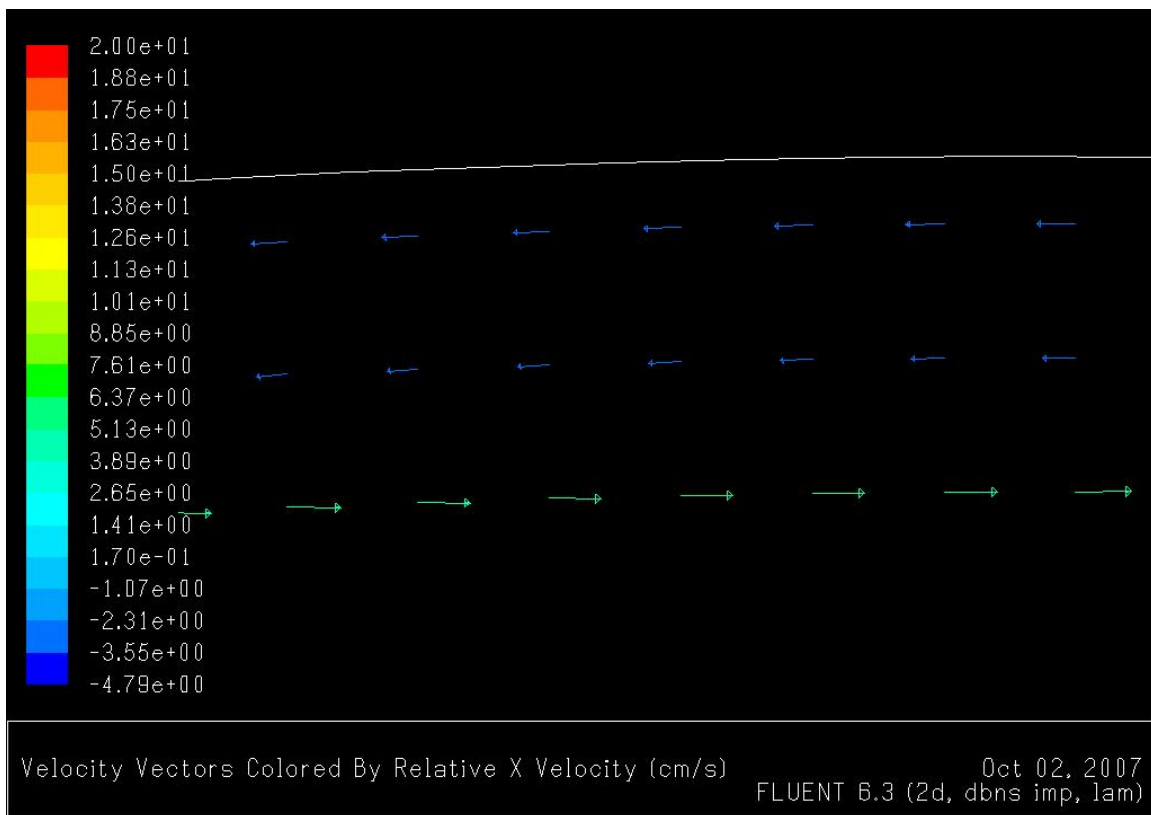


Figure 6.7. Plate 1, Velocity Vectors, Oil, Re = 100

The similar cases were simulated with plates with phase angle of 45° and 90° with each other. Velocity contours for the plate with phase angle of 45° is shown in figure 6.8. The region with blue shade which is near the walls is the low velocity region some of which has some reversed flow. The maximum value of the reversed flow is 0.768 m/s which is low when you consider the inlet velocity is 7.45 m/s . The maximum velocity (11.6 m/s) too is less in proportion to inlet velocity when compared to the case where there was no offset between the plates. This can be attributed to the fact that the difference between the maximum and minimum spacing between the plates in this case is much lesser than when the plates are aligned with each other.

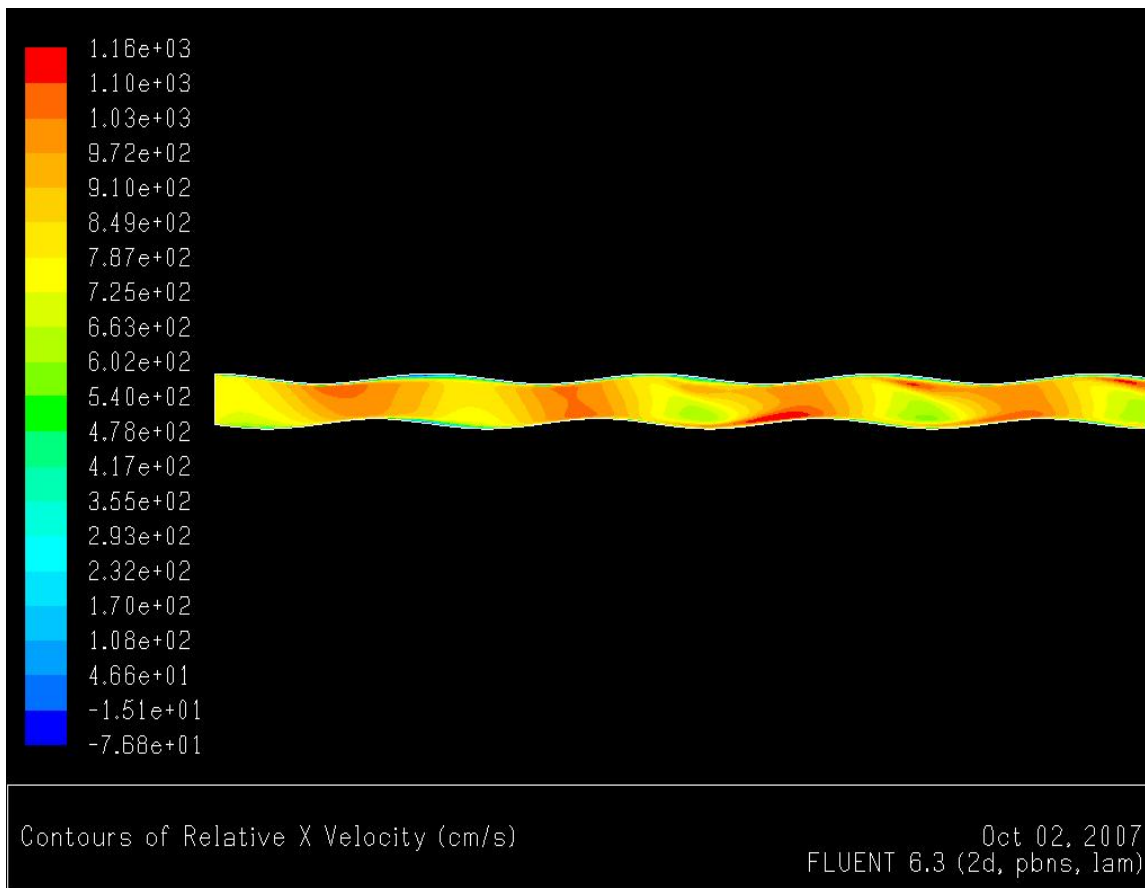


Figure 6.8. Velocity Contours, phase 45° , Oil, $a = 0.0022$, $\lambda = 0.1016$, $Re = 1000$

When the plates are offset by 90° it was observed that there were no recirculation zones. The inlet velocity was 8.44 m/s and the maximum velocity was 9.58 m/s near the end of the channel. So there is hardly any acceleration of the flow. The minimum velocity of the flow was 1.31 m/s near the top wall.

6.2 Plate 2

The velocity contours of the plate 2 are shown in figure 6.9. The fluid used is blood. The phase angle between the plates is 0° .

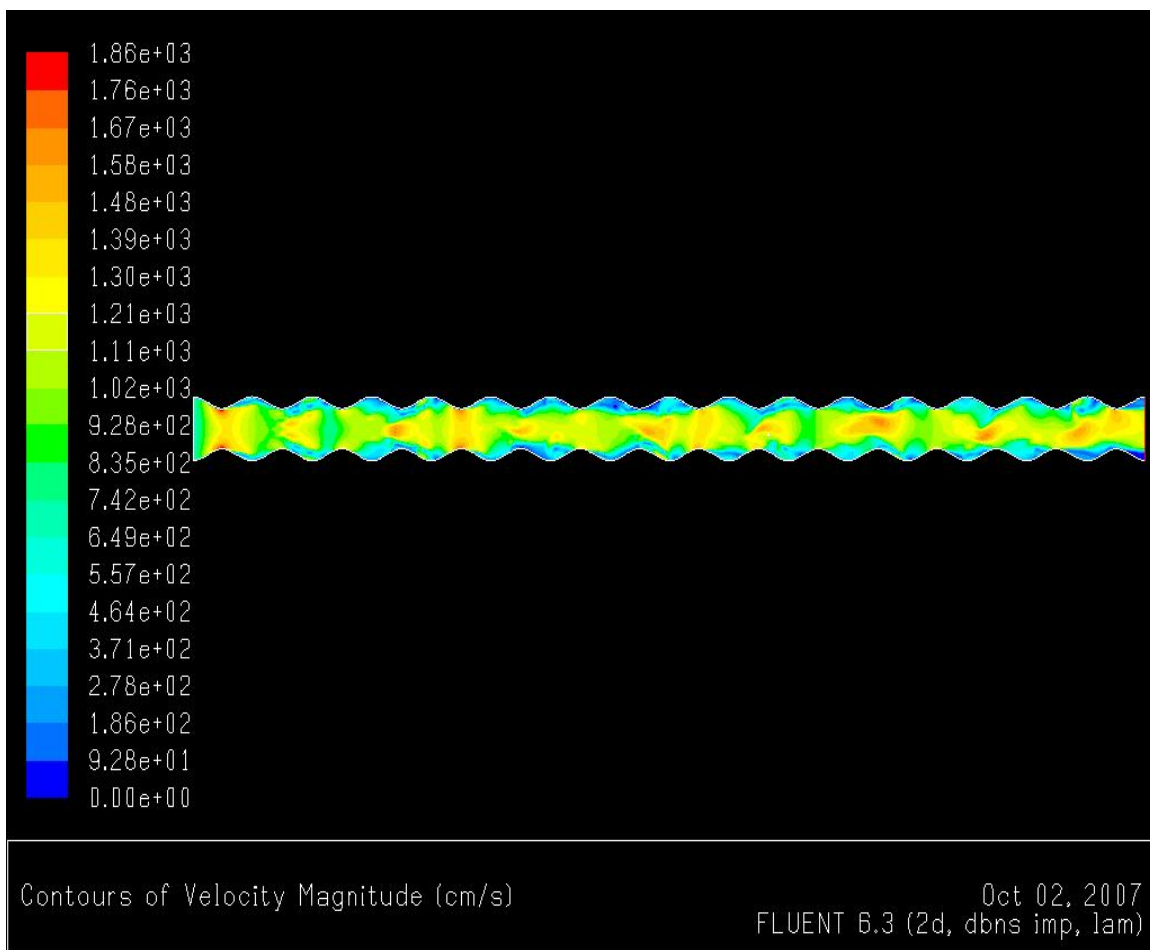


Figure 6.9. Velocity Contours, Oil, $a = 0.0022$, $\lambda = 0.0254$, $Re = 1000$

Seen in the figure below is the plot for the centerline velocity for the same case. The inlet velocity of the flow is 6.97 m/s and the maximum velocity is 16.15 m/s. which is a little more when compared to the same case of plate 1. Plate 2 has a smaller wavelength when compared to plate 1.

The center line velocity along the length of the channel is shown in figure 6.10.

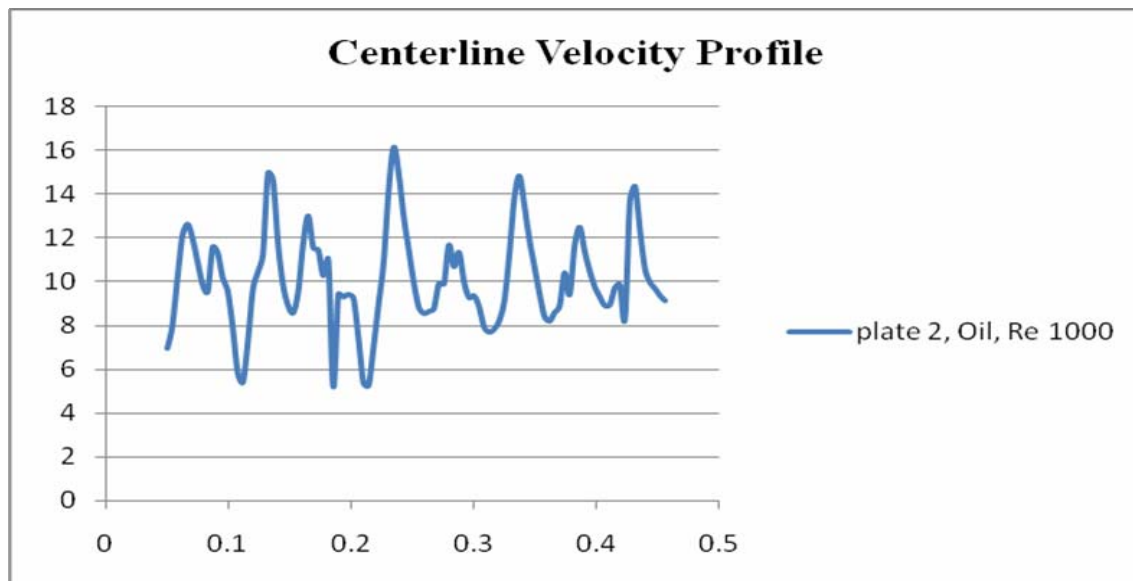


Figure 6.10. Plate 2, Centerline Velocity Profile

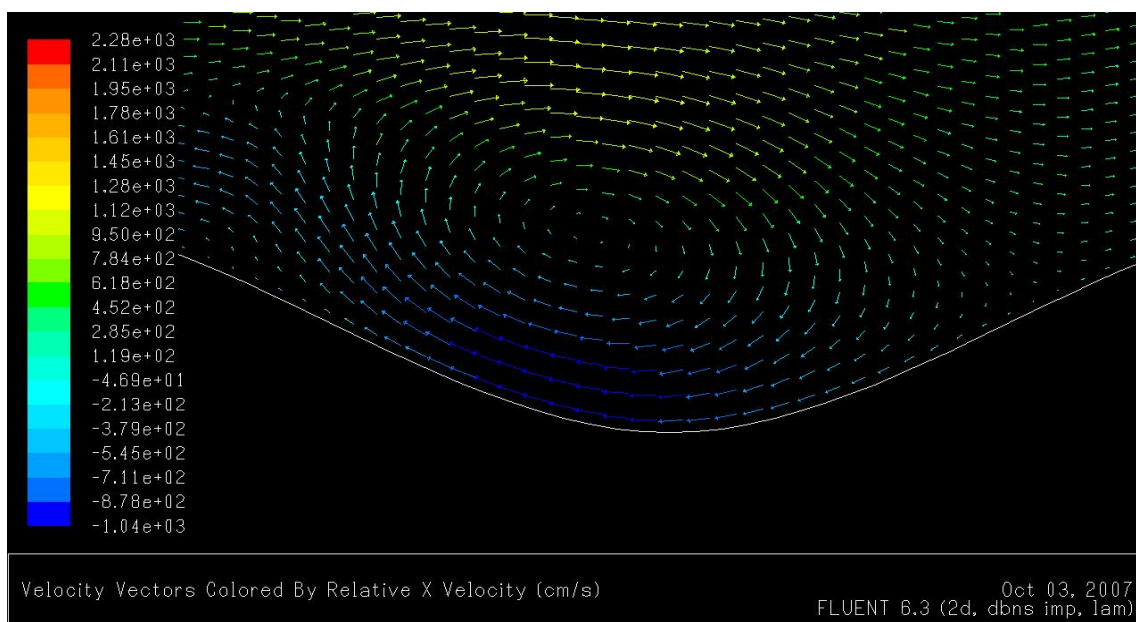


Figure 6.11. Velocity Vectors, Phase 0, Oil, $a = 0.0022$, $\lambda = 0.0254$, $Re = 1000$

The velocity vectors near the bottom plate are shown in figure 6.11. There are a lot of high velocity reversed flow regions in the flow. The maximum velocity of the reversed flow is 10.4 m/s, which is 60% greater than the inlet velocity.

It is observed that when the wavelength is reduced by keeping the amplitude constant, there is more reversed flow and also the velocity of the reversed flow is higher. The same trend was observed when blood was used as the fluid.

The simulations were repeated for plate 2 with phase difference of 45° and 90° between the plates. Shown below are the velocity contours for plate 2 with a phase difference of 90° between the plates. It can be seen in figure 6.12 that the fluid accelerates quite a bit more than plate 1. The inlet velocity is 8.47 m/s and the maximum velocity is 12.33 m/s. This happens even though the cross section area does not change anywhere between the plates. It can be observed in figure 6.13 that there is a small region of reversed flow. This is a possible reason for the flow to accelerate. The maximum velocity of this reversed flow is 1.4 m/s, which is about $1/6^{\text{th}}$ of the inlet velocity.

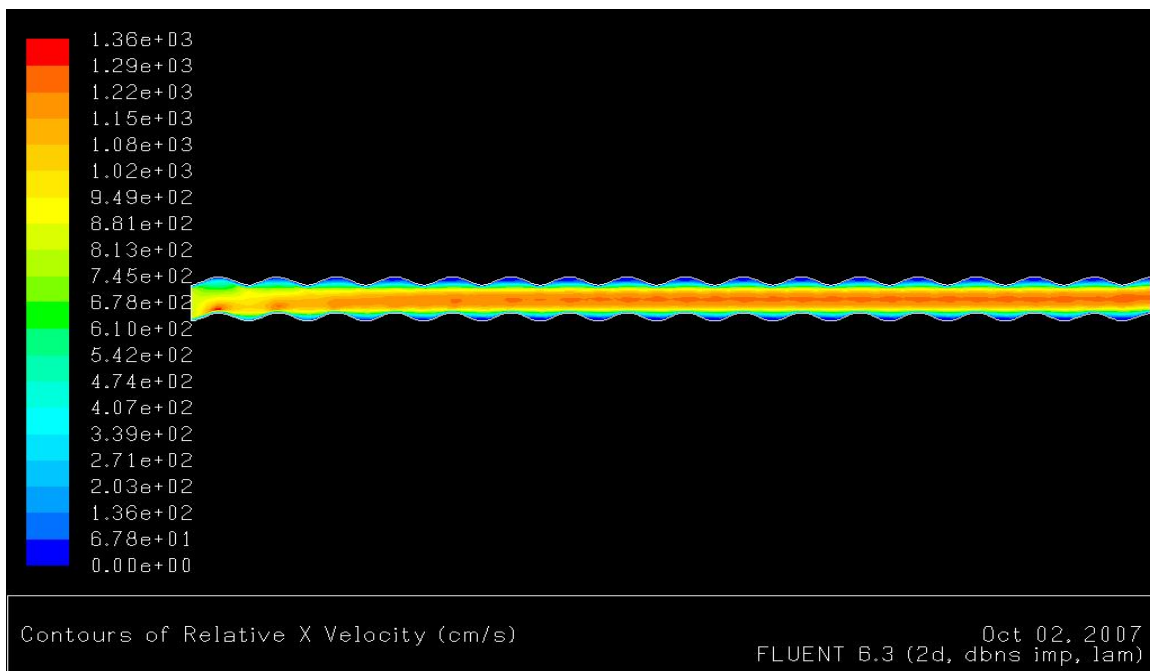
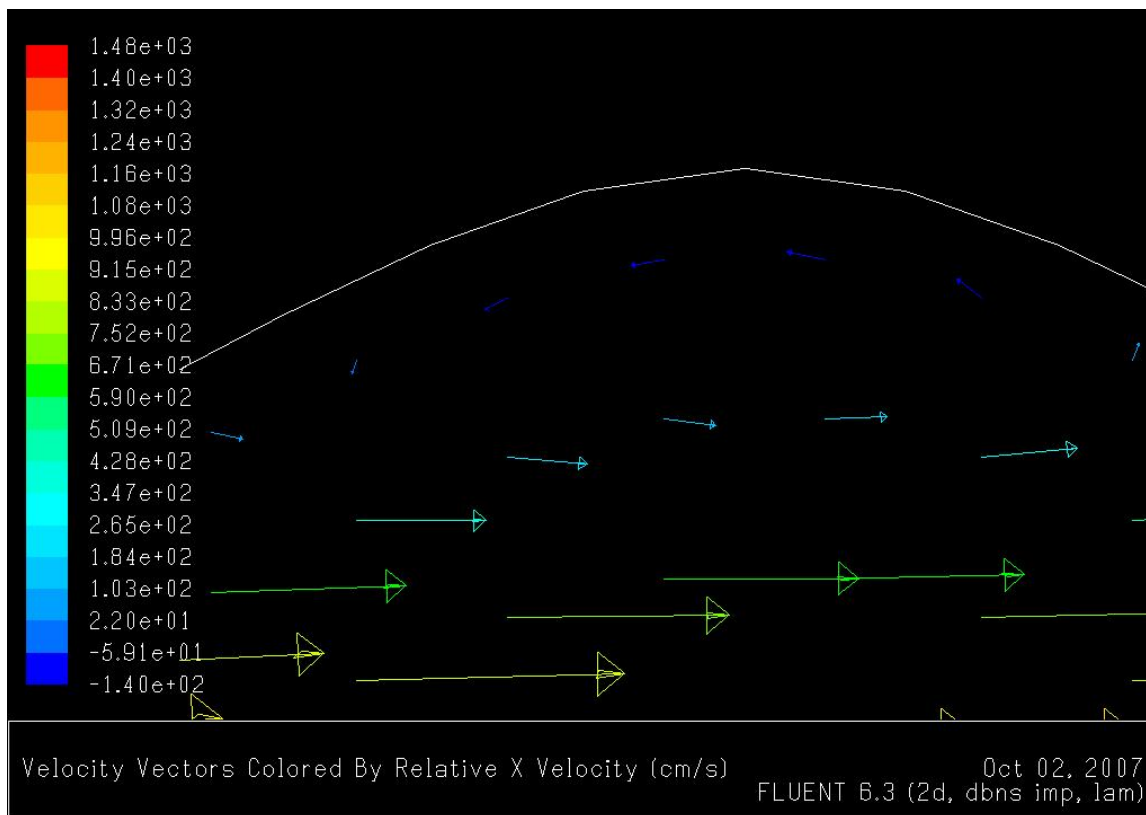


Figure 6.12. Velocity Contours, Phase 90, Oil, $a = 0.0022$, $\lambda = 0.0254$, $Re = 1000$ Figure 6.13. Velocity Vectors, Phase 90, Oil, $a = 0.0022$, $\lambda = 0.0254$, $Re = 1000$

6.3 Plate 3

In plate 3 the amplitude is reduced to 0.0005 m but wavelength is the same as plate 2. It was observed that there was reversed flow only for the case where oil was used as the fluid and the Reynolds number was 1000. The velocity contours for such a case is shown in figure 6.14. The flow accelerated to 9.43 from the inlet velocity of 6.85. From the velocity vectors in figure 6.15 it can be seen that there is very little reversed flow and it has a maximum value of 0.9 m/s.

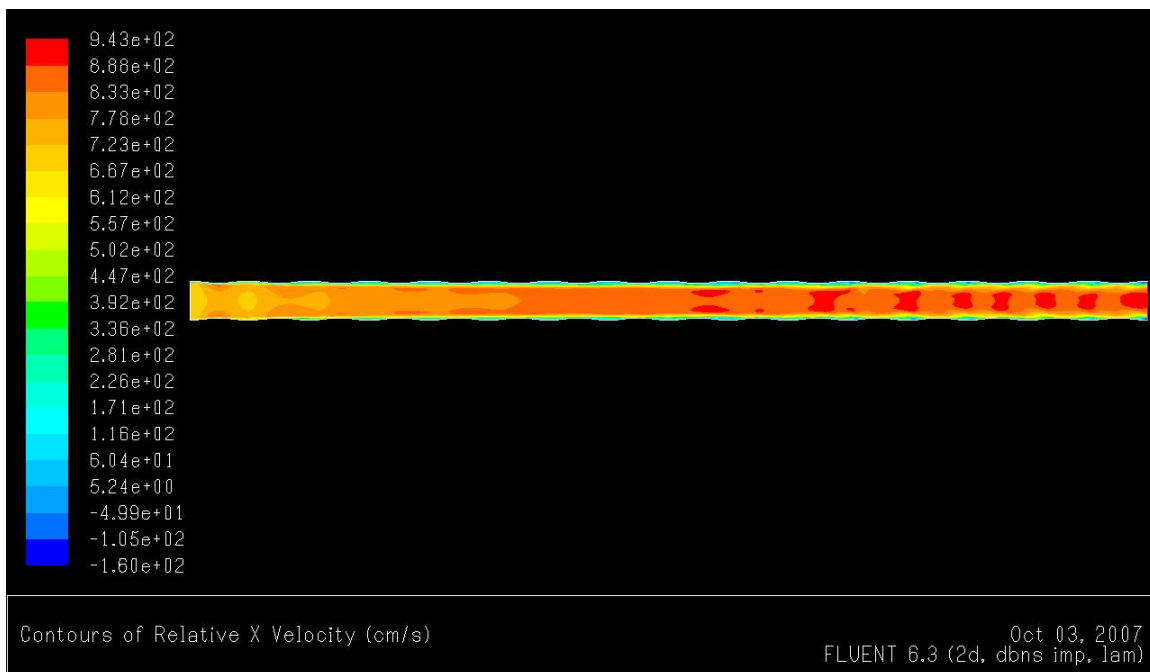


Figure 6.14. Velocity Contours, Phase 0, Oil, $a = 0.0005$, $\lambda = 0.0254$, $Re = 1000$

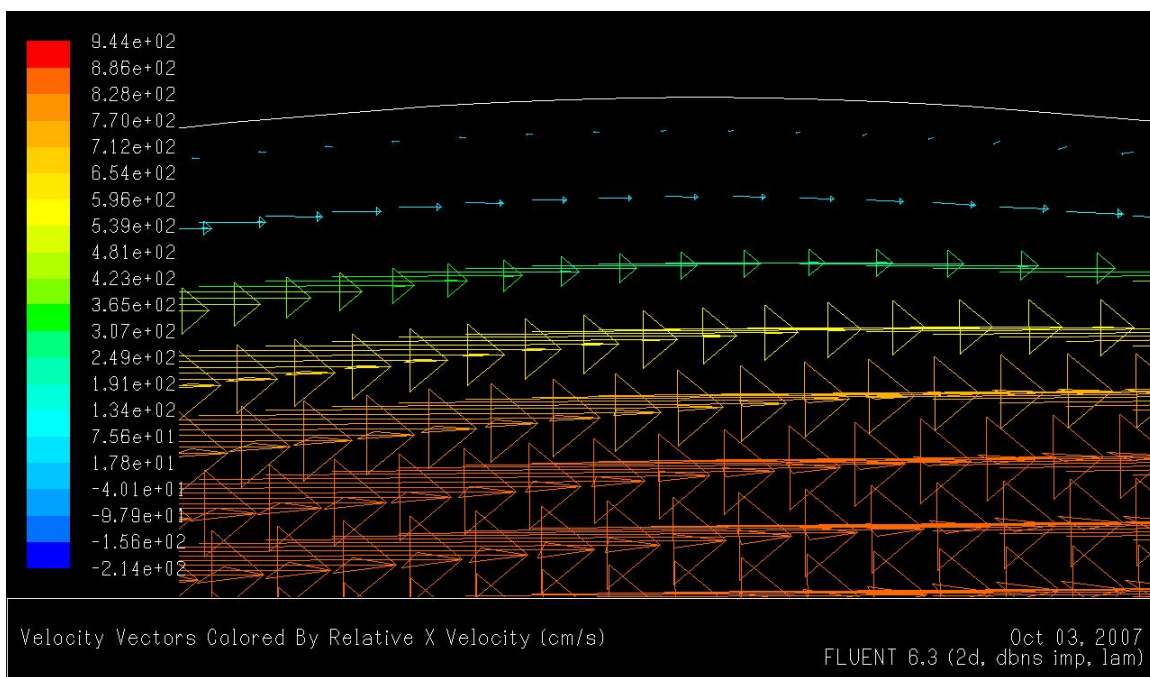


Figure 6.15. Velocity Vectors, phase 0, Oil, $a = 0.0005$, $\lambda = 0.0254$, $Re = 1000$

6.4 Plate 4

In plate 4 the amplitude is 0.0044 m which is twice the value than for plate 1 but the wavelength is 0.1016 m which is the same as plate 1. The inlet velocity for a Reynolds number of 1000 and without offset is 6.83 m/s. The velocity vectors for such a case are shown in figure 6.16. The maximum velocity of the flow is 21.5 m/s, which is about 3 times the value at the inlet. There are lots of recirculation zones in the flow like the one seen below. The maximum value of the velocity of the reversed flow is 12.4 m/s which is twice the value at the inlet.

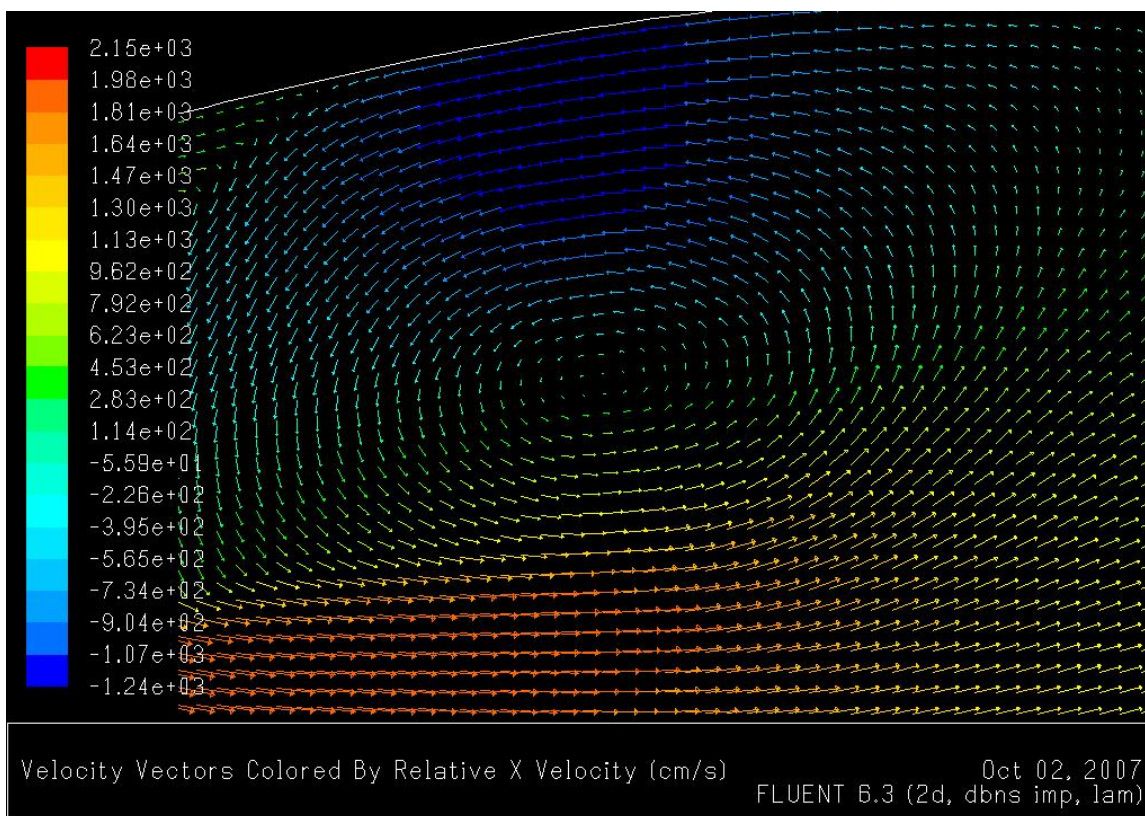


Figure 6.16. Velocity vectors, phase 0, Oil, $a = 0.0044$, $\lambda = 0.1016$, $Re = 1000$

Shown in figure 6.17 is the plot of the centerline velocity along the length of the channel.

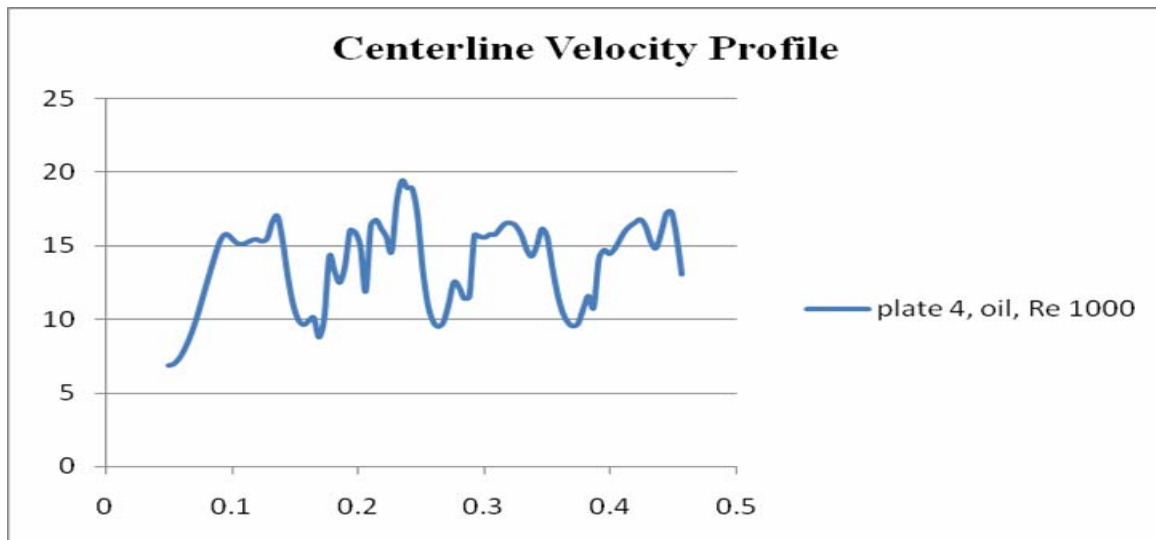


Figure 6.17. Plate 4, Centerline Velocity Profile

The figure 6.18 shows the velocity vectors for oil for a Reynolds number of 100. Recirculation zones can be clearly seen, which have a maximum magnitude of 1.1 m/s compared to the inlet velocity of 0.68 m/s. The flow is accelerated all the way to a velocity of 2.25 m/s which is about 3.5 times the inlet velocity.

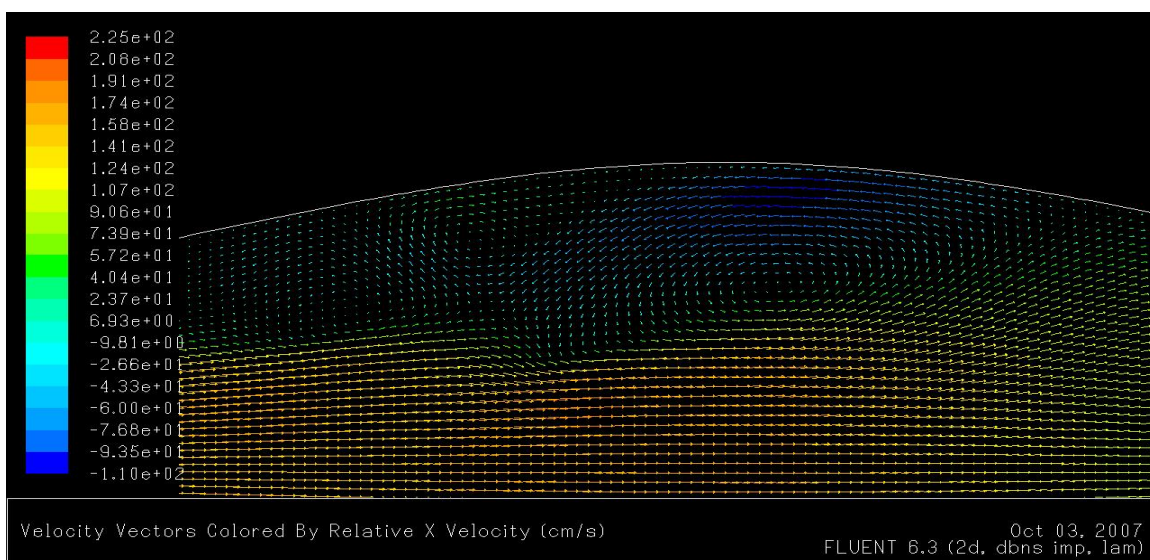


Figure 6.18. Velocity Vectors, Oil, $a = 0.0044$, $\lambda = 0.1016$, $Re = 100$

The simulations were repeated for plate 4 with phase difference of 45° and 90° between the plates. Shown below in figure 6.19 are the velocity contours for plate 4 with a phase difference of 45° between the plates. The maximum velocity of the flow is 15.6 m/s.

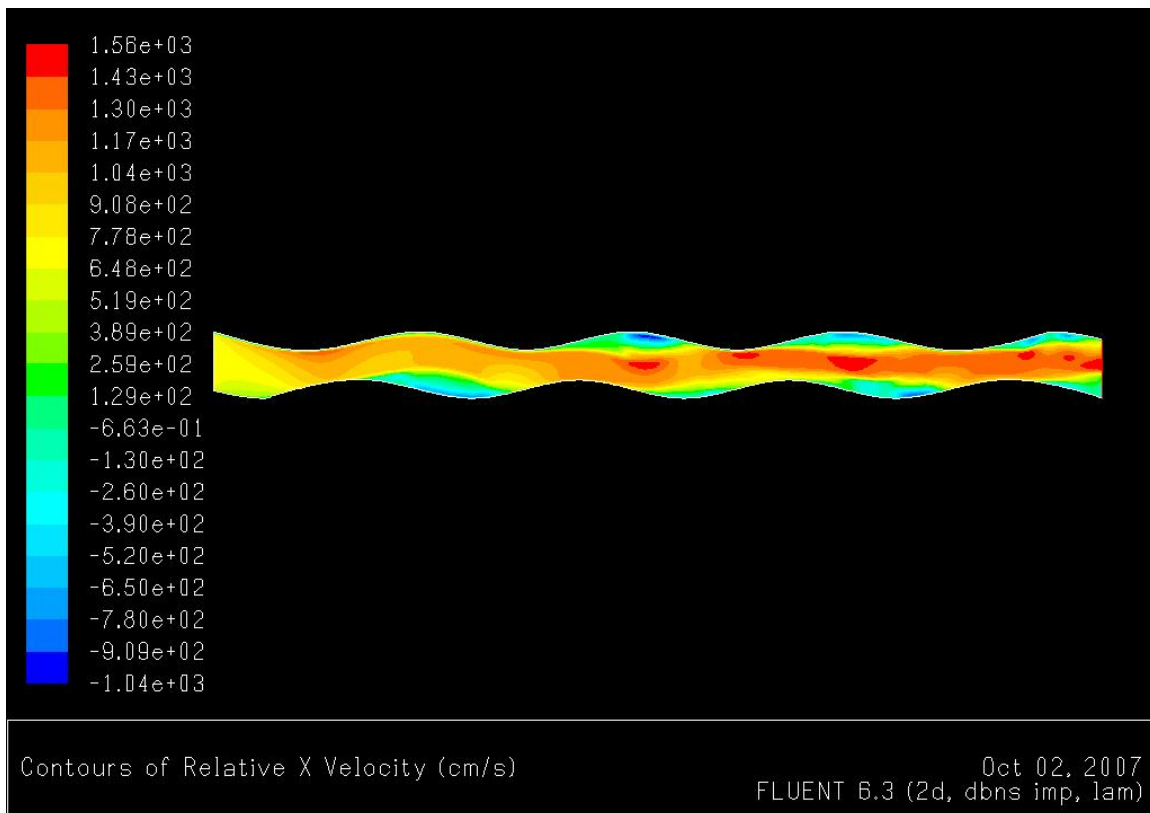


Figure 6.19. Velocity vectors, phase 45° , Oil, $a = 0.0044$, $\lambda = 0.1016$, $Re = 1000$

Shown in figure 6.20 are the velocity vectors for the same case. The recirculation zones can be clearly seen. The maximum velocity of the reversed flow is 10.8 m/s while the inlet velocity is 6.84 m/s .

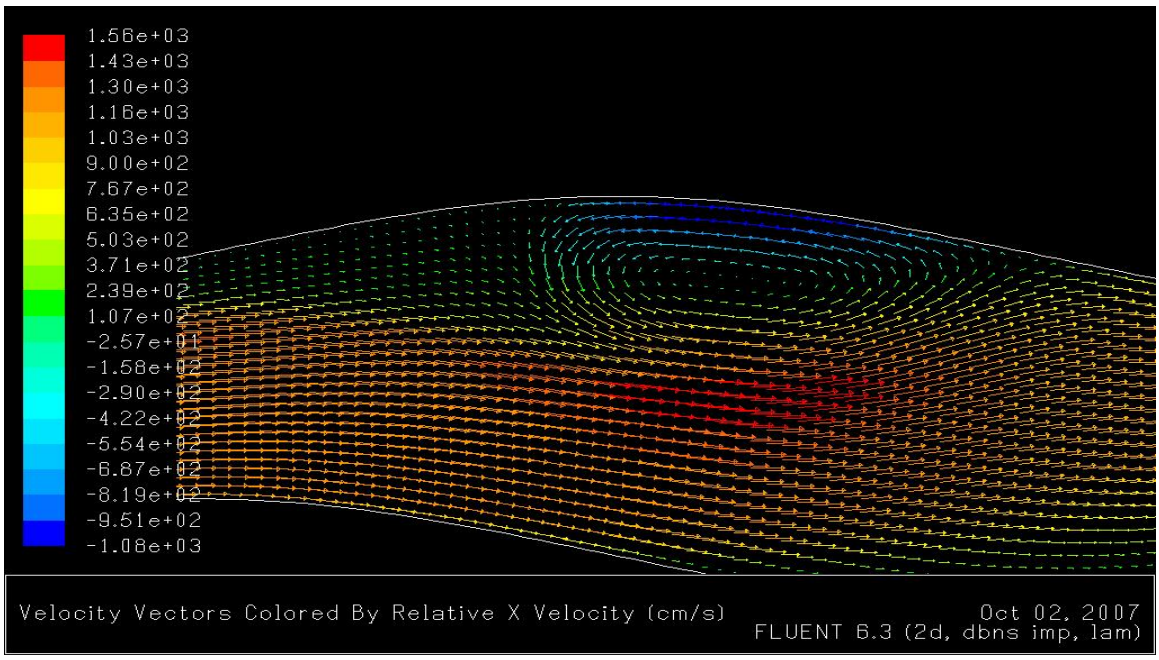


Figure 6.20. Velocity Vectors, Phase 45°, Oil, $a = 0.0044$, $\lambda = 0.1016$, $Re = 1000$

Shown below in figure 6.21 are the velocity contours for a similar case as above except that the phase difference between the plates is 90°.

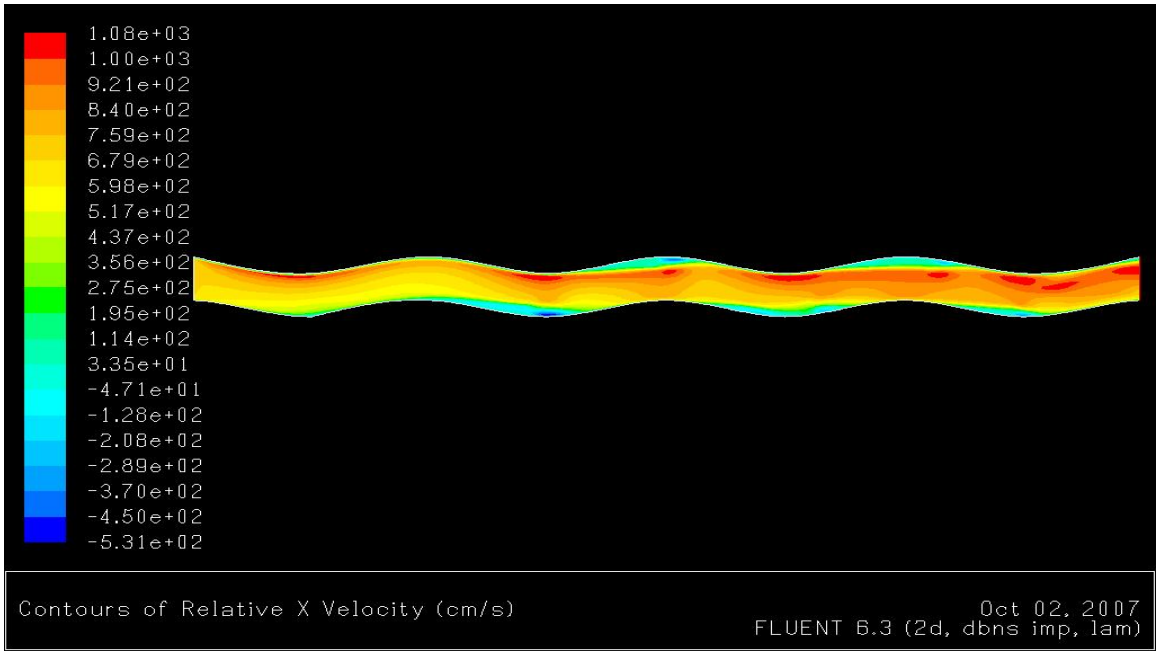


Figure 6.21. Velocity Vectors, Phase 90°, Oil, $a = 0.0044$, $\lambda = 0.1016$, $Re = 1000$

It can be seen in figure 6.22 that there is acceleration in the flow even though there is no change in the cross section of the channel. This can be attributed to the reversed flow as seen in the figure below. This figure shows the velocity vectors. The reversed flow can be clearly seen. The maximum velocity of the reversed flow is 5.79 m/s even though the inlet velocity is 6.84 m/s.

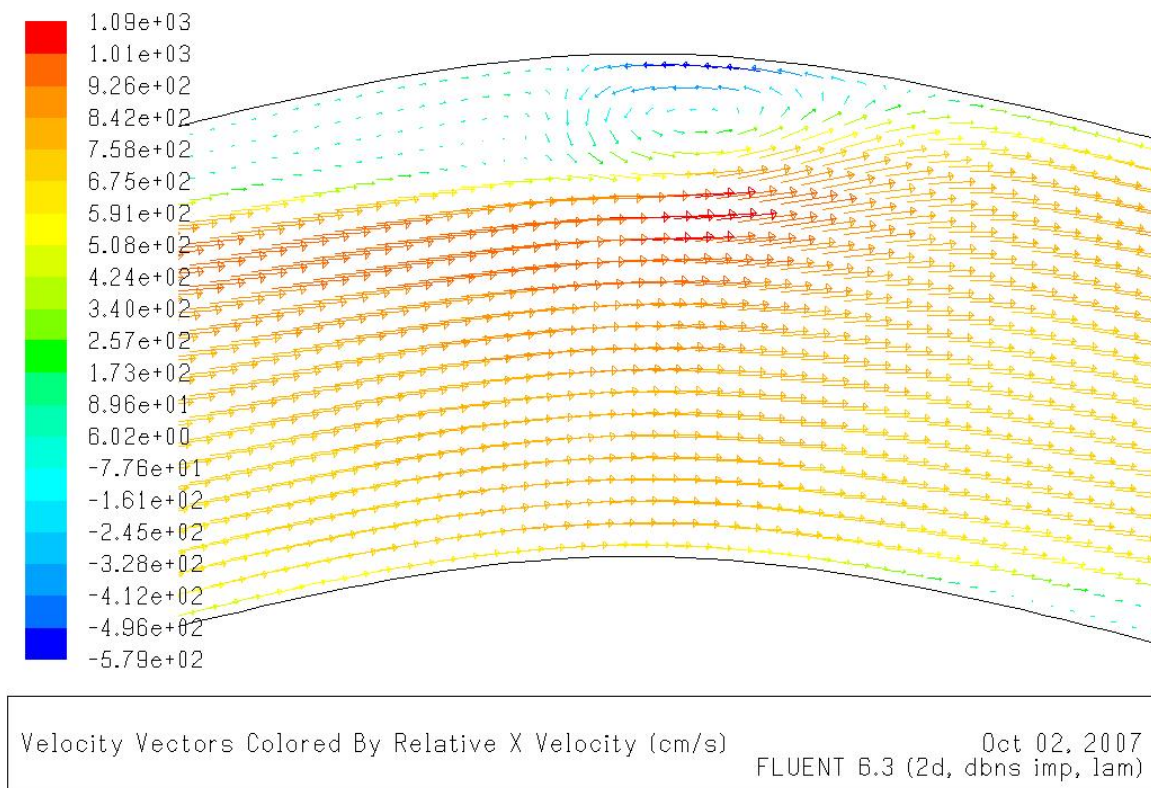


Figure 6.22. Velocity vectors, phase 90° , Oil, $a = 0.0044$, $\lambda = 0.1016$, $Re = 1000$

Shown in figure 6.23 are the velocity vectors for blood for a Reynolds number of 1000 with the plates 90° out of phase with each other. Reversed flow was observed in this case although it cannot be clearly seen in this figure. Even though the inlet velocity is only 0.41 m/s and there is no change in the cross section area of the channel there are reversed flows.

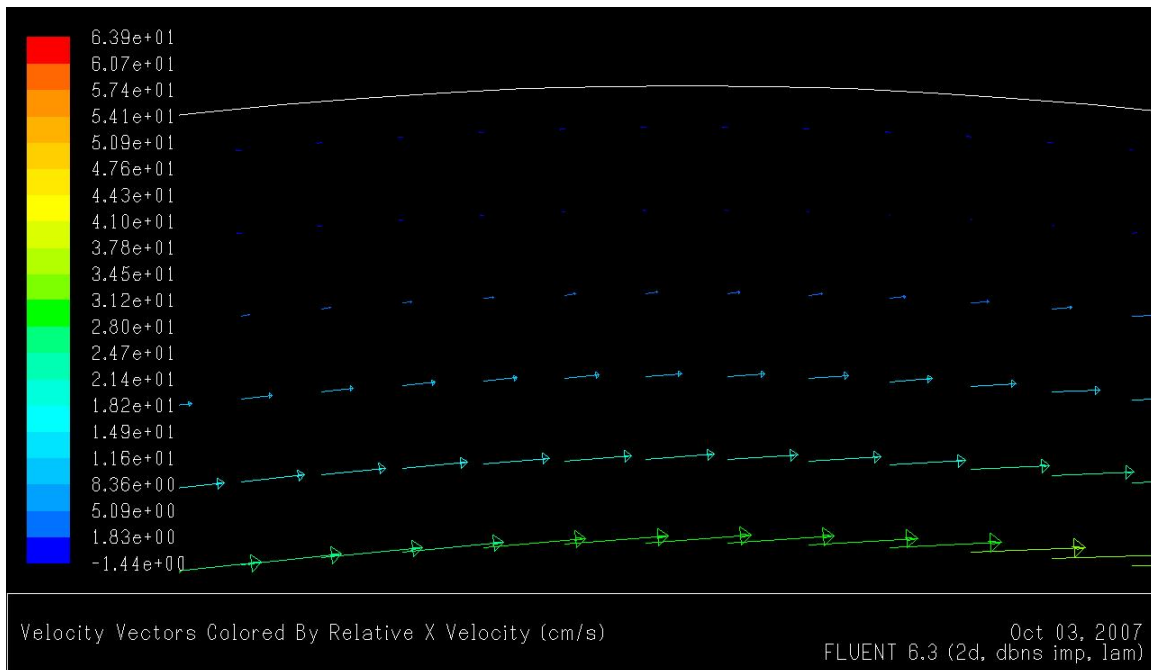


Figure 6.23. Velocity vectors, phase 90° , Blood, $a = 0.0044$, $\lambda = 0.1016$, $Re = 1000$

It can be observed that when the amplitude is increased with the wavelength kept the same, there is an increase in the reversed flow and the reversed flow velocity.

REFERENCES

- [1] B. Anglade and R. Khayat, "Pattern formation in weakly forced Taylor–Couette flow of viscoelastic fluids," *Journal of Non-Newtonian Fluid Mechanics*, vol. 130, no. 1, pp. 29–44, 2005.
- [2] H. M. S. Bahaidarah, N. K. Anand and H. C. Chen, "Numerical study of heat and momentum transfer in channels with wavy walls," *Numerical Heat Transfer, Part A*, vol. 47, pp. 417-439, 2005.
- [3] J. M. Broadbent, A. Kaye, A.S. Lodge and D.G. Vale, "Possible systematic error in the measurement of normal stress difference in polymer solutions in steady shear flow," *Nature*, vol. 217, pp. 55-56, 1968.
- [4] J. A. Deiber and W. R. Schowalter, "Flow through tubes with sinusoidal axial variations in diameter," *AIChE J.*, vol. 25, pp. 638-644, 1979.
- [5] J. A. Deiber and W. R. Schowalter, "Modeling the flow of Viscoelastic fluids through porous media," *AIChE J.*, vol. 27, pp. 912-920, 1981.
- [6] J. Hron, J. Malek, and S. Turek, "A numerical investigation of flows of shear-thinning fluids with applications to blood rheology," *International Journal for Numerical Methods in Fluids*, vol. 32, no. 7, pp. 863–879, 2000.
- [7] D. F. James, N. Phan-Thien M.M.K. Khan, A.N. Beris and S. Pilitsis, "Flow of test fluid MI in corrugated tubes," *Journal of Non-Newtonian Fluid Mechanics*, vol. 35, pp. 405-412, 1990.
- [8] D. F. James and D. R. McLaren, "The laminar flow of dilute polymer solutions through porous media," *J. Fluid Mech.*, vol. 70, pp. 733 752, 1975.

- [9] T. Lee, "Numerical study of fluid flow through double bell-shaped constrictions in a tube," *International Journal of Numerical Methods for Heat & Fluid Flow*, vol. 12, no. 2, pp. 258–289, 2002.
- [10] S. Muller, "Velocity measurements in complex flows of non-Newtonian fluids," *Korea-Aust Rheo. J*, vol. 14, pp. 93–105, 2002.
- [11] N. Phan-Thein and M. M. K. Khan, "Flow of an Oldroyd-type fluid through a sinusoidally corrugated tube," *Journal of Non-Newtonian Fluid Mechanics*, vol. 24, pp. 203-220, 1987.
- [12] N. Phan-Thien and M. M. K. Khan, "Flow of an Oldroyd-type fluid through a sinusoidally corrugated tube," *J. Non-Newtonian Fluid Mech.*, vol. 24, pp. 203- 220, 1987.
- [13] K. R. Rajagopal and A. Mir-Mohamad-Sadegh, "A boundary integral approach for determining the pressure error," *Rheol. Acta*, vol. 19, pp. 12- 18, 1980.
- [14] W. H. Schwarz and C. Bruce, "Rheological properties of ionic and nonionic polyacrylamide solutions," *J. Polym. Sci.*, vol. 7, pp. 909-927, 1969.
- [15] R. Sureshkumar, "Local linear stability characteristics of viscoelastic periodic channel flow," *Journal of Non-Newtonian Fluid Mechanics*, vol. 97, no. 2-3, pp. 125–148, 2001.
- [16] R. C. Yalamanchili, A. Sirivat and K. R. Rajagopal, "An experimental investigation of the flow of dilute polymer solutions through corrugated channels," *Journal of Non-Newtonian Fluid Mechanics*, vol. 58, pp. 243-277, 1995.
- [17] R. C. Yalamanchili, "Flow of non-Newtonian fluids in corrugated channels," *Journal of Non-Linear Mechanics*, vol. 28, no. 5, pp. 535-548, 1993.

VITA

Rohit Aiyalur Shankaran was born in Hyderabad, India. He received his Bachelor of Engineering degree in mechanical engineering from Osmania University, Hyderabad in June 2005 and his Master of Science Degree in mechanical engineering from Texas A&M University, College Station in December 2007.

Rohit may be reached by mail at 405 Cherry Street, Apt 2, College Station, Texas, 77840 or by email at rohit_as86@yahoo.com.

The typist for this thesis was Rohit Aiyalur Shankaran.